Quaternary Science Reviews 238 (2020) 106282

Contents lists available at ScienceDirect

Quaternary Science Reviews

journal homepage: www.elsevier.com/locate/quascirev

Taguatagua 1: New insights into the late Pleistocene fauna, paleoenvironment, and human subsistence in a unique lacustrine context in central Chile

Rafael Labarca [a, b, *], Erwin González-Guarda [b, c, d], Álvaro Lizama-Catalán [b, e], Natalia A. Villavicencio [b, f, g], Jhonatan Alarcón-Muñoz [b, h], Felipe Suazo-Lara [b, h], Pablo Oyanadel-Urbina [b, i], Paula Soto-Huenchuman [b, h, j], Christian Salazar [b, k], Sergio Soto-Acuña [b, h], Karina E. Buldrini [b, l]

[a] Escuela de Arqueología and Transdisciplinary Center for Quaternary Research (TAQUACH), Universidad Austral de Chile, Los Pinos s/n, Balneario Pelluco, Puerto Montt, Chile
[b] Corporación Laguna de Taguatagua, Av. Libertador Bernardo O'Higgins 351, Santiago, Chile
[c] Instituto de Ciencias Sociales, Universidad de O'Higgins, Av. Libertador Bernardo O'Higgins 611, Rancagua, Chile
[d] Biomolecular Laboratory, Institut Català de Paleoecologia Humana i Evolucio Social, 43007, Tarragona, Spain
[e] Departamento de Antropología, Facultad de Ciencias Sociales, Universidad de Chile, Av. Ignacio Carrera Pinto, 1045, Santiago, Chile
[f] Departamento de Ecología, Facultad de Ciencias Biológicas, Pontificia Universidad Católica de Chile, Av. Libertador Bernardo O'Higgins 340, Santiago, Chile
[g] Instituto de Ecología y Biodiversidad, Las Palmeras, 3425, Santiago, Chile
[h] Red Paleontológica U-Chile, Laboratorio de Ontogenia y Filogenia, Facultad de Ciencias, Universidad de Chile. Las Palmeras, 3425, Ñuñoa, Santiago, Chile
[i] Laboratorio de Paleobiología, Centro de Estudios Avanzados en Zonas Áridas. Ossandon 877, Coquimbo, Chile
[j] Consultora Paleosuchus Ltda., Huelen 165 Depto C, Santiago, Chile
[k] Escuela de Geología, Facultad de Ingeniería, Universidad del Desarrollo, Av. La Plaza 680, Santiago, Chile
[l] Área de Zoología de Vertebrados, Museo Nacional de Historia Natural de Chile, Casilla 787, Santiago, Chile

ARTICLE INFO

Article history:
Received 11 October 2019
Received in revised form
25 February 2020
Accepted 30 March 2020
Available online 11 May 2020

Keywords:
Pleistocene
South America
Megafauna
Small fauna
Taphonomy
Paleoenvironment

ABSTRACT

The Laguna de Tagua Tagua has yielded two important late Pleistocene archaeological sites, Taguatagua 1 and Taguatagua 2, in which a clear early human exploitation of megafauna has been recorded. Particularly in Taguatagua 1 (TT-1), here re-dated around 12,600 cal yr BP, an abundant small faunal assemblage was also recovered, which had not been previously studied in detail. Here we report the first comprehensive taxonomic and taphonomic analysis of this site. We identified 28 different taxa, including mollusks, fish, anurans, reptiles, birds, marsupials, rodents, carnivores, gomphotheres, horses and cervids, making this the richest late Pleistocene site in Chile so far. Among these, sixteen taxa are new for the Chilean late Pleistocene. Birds are the richest group, with ten taxa, followed by rodents with eight taxa. Most of the species currently inhabit the area, but we identified some locally extirpated taxa, together with extinct taxa (exclusively megamammals). Taphonomic analysis suggests a very complex depositional scenario, mostly related to lake-level oscillations which covered and exposed a mainly natural deposited small faunal assemblage. So far, we detected human-made modifications exclusively in horse and cervid bones. Current habitat requirements of the extant fauna, as well as dietary reconstruction of extinct fauna, suggest a highly variable climate and vegetation during the formation of TT-1 since taxa with preferences from semiarid to humid/wooded environments were identified. These results can be related to the changes from cold/wet to dry/warm conditions documented during the Pleistocene - Holocene transition.

1. Introduction

The late Pleistocene (~126–11,7 kyr) faunal record in central Chile (~32–35°) is abundant, with around 32 paleontological and/

* Corresponding author. Escuela de Arqueología and Transdisciplinary Center for Quaternary Research (TAQUACH), Universidad Austral de Chile, Los Pinos s/n, Balneario Pelluco, Puerto Montt, Chile.
E-mail address: rafael.labarca@uach.cl (R. Labarca).

https://doi.org/10.1016/j.quascirev.2020.106282
0277-3791/

or archaeological sites scattered along coastal areas, the Coastal range, the intermediate depression and the pre Andean range (Frassinetti and Alberdi, 2000; Labarca, 2015; and references therein). However, most of the fossils known at present come from fortuitous findings without detailed stratigraphic or contextual information. Due to this, the paleontological faunal record is widely dominated by easy-to recover taxa, particularly by gomphotheres and horses (Casamiquela, 1976, 1999; Cartajena et al., 2013; Labarca, 2015; Labarca et al., 2016; Núñez et al., 1994) from which initial paleoecological, chronological and taxonomical work has been done (Alberdi and Frassinetti, 2000; Casamiquela, 1972; Casamiquela and Sepúlveda, 1974; Frassinetti and Alberdi, 2000; González-Guarda et al., 2018; Labarca and Alberdi, 2011; Labarca and Alcaraz, 2011; López et al., 2016). For other groups of smaller size, such as rodents, marsupials, reptiles, anurans, fish and birds, the information is sparse and, in some cases, non-existent. This marked imbalance has prevented an adequate reconstruction of late Pleistocene faunal assemblages in central Chile, a problem that could be partially solved with the study of deposits located in different geological settings with a high faunal richness and well-controlled stratigraphic and chronological context. In this scenario, this paper presents the extraordinary faunal record of Taguatagua 1 (TT-1), an archaeo-paleontological site located in the Coastal Range of central Chile (Fig. 1), dated around 12,600 cal yr BP. At this site, a clear association between cultural remains and a particularly rich faunal assemblage in a lacustrine environment has been documented (Casamiquela, 1976; Montané, 1968; Núñez et al., 1994; Palma, 1969), offering a unique opportunity to address not only taxonomic issues, but also discuss the taphonomic processes involved, human exploitation of different taxa and paleoenvironmental reconstruction during late glacial times. The present contribution has three main goals. First, to report the results of the taxonomic study of the fossils recovered at the TT-1 site. This faunal assemblage corresponds to the richest described for the late Pleistocene of Chile until now, and significantly increases the knowledge about the continental faunas of the late Quaternary in Chile and southern South America. The fossil assemblage does not only contain taxa of very different taxonomic groups (Placentalia, Marsupialia, Aves, Serpentes, Lissamphibia, Osteichthyes, Mollusca) but also includes a large number of species of which there was no fossil record in the area, some of them locally extirpated. Second, to present a qualitative taphonomical analysis centered mainly on bone modifications. In this line of research, a complex pre and post burial history is suggested, in which a time-averaged shore-lake natural bone deposition was disturbed by an ephemeral human occupation centered in megamammals exploitation. Third, to explore this faunal context as a paleoenvironmental proxy, in order to improve the understanding of the Pleistocene – Holocene transition at a locality level in central Chile.

2. Site context

2.1. Geographic location and geological setting

The studied material was sampled from the Laguna de Tagua Tagua Formation (LTTF) (Upper Pleistocene to Holocene), located in the Laguna de Tagua Tagua locality (LTT), a former lake artificially drained in the XIX century (Núñez et al., 1994). The LTTF corresponds to Cenozoic lacustrine units contained in the oriental margin of the Coastal Range (Fig. 1A1-2). The older lithological units in the area correspond to La Lajuela Formation (*sensu* Soto-Huenchuman, 2018) assigned to the Tithonian–Berriasian, Las Chilcas Formation (Barremian-Albian), the Alhué Plutonic Complex (Albian-Cenomanian) and restricted contact metamorphic rocks (Godoy et al., 2009) (Fig. 1A3).

LTTF is defined as a 12.6 m thick assemblage of semi-consolidated fine sediments, such as clay and silt, unconformably overlaying to tuff layers (Varela, 1976) assigned to the Pudahuel Ignimbrite unit by Lara et al. (2008), extended over a surface of 120 km^2 approximately, into tectonic graben. The top of the LTTF is exposed as the current surface or recent soil (Godoy et al., 2009; Varela, 1976).

Varela (1976) divided the formation in eight members, member 1 (12.62–11.37 m) is composed of massive sand and gravel of alluvial origin, while members 2 to 8 (11.36 m-to surface) are composed of lacustrine greenish, brownish and grayish massive to laminated clays and silts with some diatomaceous inclusions, especially at the top of the sedimentary accumulation (Fig. 1B1). Latter sedimentological studies carried out by Valero-Garcés et al. (2005) defined a new succession composed for nine units, which partially correlates with Varela's original description.

The TT-1 archaeo-paleontological site is located at the unconformity between member 5 and member 6, at around 2.4 m depth (Fig. 1B2). The cultural materials and faunal remains were mainly recovered at the base of member 6 in which a discontinuous paleosoil was detected, but also at the top of the member 5 (Varela, 1976).

2.2. Chronology

Based on extrapolated sedimentation rates, Varela (1976) suggested an age older than 51,000 yr BP for the bottom of the LTTF. Valero-Garcés et al. (2005) obtained a date of ~42,000 yr BP from the base of his Unit 8 (member 3 according to Varela, 1976), which is located 7 m depth (Fig. 1B). Since the Pudahuel Ignimbrite unit is dated around 150,000 yr BP (Lara et al., 2008), the LTTF can be assigned with confidence to the Upper Pleistocene to Holocene.

With regards to TT-1, Montané (1968) reports a date of 13,200 cal yr BP (GX-1205: 11,380 ± 20) on charcoal. A duplicate of the same sample gave a date of 12,860 cal yr BP (Gif-1265: 11,000 ± 250, Palma, 1969). Considering that the dates reported for TT-1 are the result of analyses performed during the early stages of development of radiocarbon dating techniques, we obtained two new dates from materials recovered during the second excavation at TT-1 (see section 2.4). The samples dated are a fragment of charred megafauna bone (D-AMS 034867, 10,578 ± 48) and a isolated charcoal sample (D-AMS 034868, 10,738 ± 43) recovered in sediments coming from the late Pleistocene archaeological level reported by Nuñez et al. (1994) (excavation units C3–F3 and C2–F3, respectively). Both new dates help to constrain this human occupation event around 12,510–12,670 cal yr BP. We have attempted to radiocarbon date gomphothere specimens from TT-1 (n = 4), but none of the samples yielded enough collagen.

Several other dates have been reported, some of which are assigned to strata closely related to the sediments from TT-1 (either top of member 5 or base of member 6). Heusser (1990) reports radiocarbon dates of 13,000 cal yr BP (RL-1954: 11,170 ± 320) and 11,290 cal yr BP (RL-1954: 9860 ± 320) from sediments located at 2.4 and 2.3 m depth, respectively, coming from his Pollen Zone 2a and 1e. On the other hand, Valero-Garcés et al. (2005) reports radiocarbon dates of 13,590 cal yr BP (Hv-23494: 11,710 ± 430) and 11,070 cal yr BP (Hv-23493: 9735 ± 270) that can be taken as bracketing dates for the interface between his Units 2 and 3 (member 5 and 6 according to Varela, 1976).

Finally, two radiocarbon dates are reported for Taguatagua 2 (TT-2), another archaeo-paleontological site located 170 m to the west from TT-1 (Núñez et al., 1994). These dates are: 11,640 cal yr BP (Beta-45520: 10,120 ± 130) and 11,310 cal yr BP (Beta-45519:

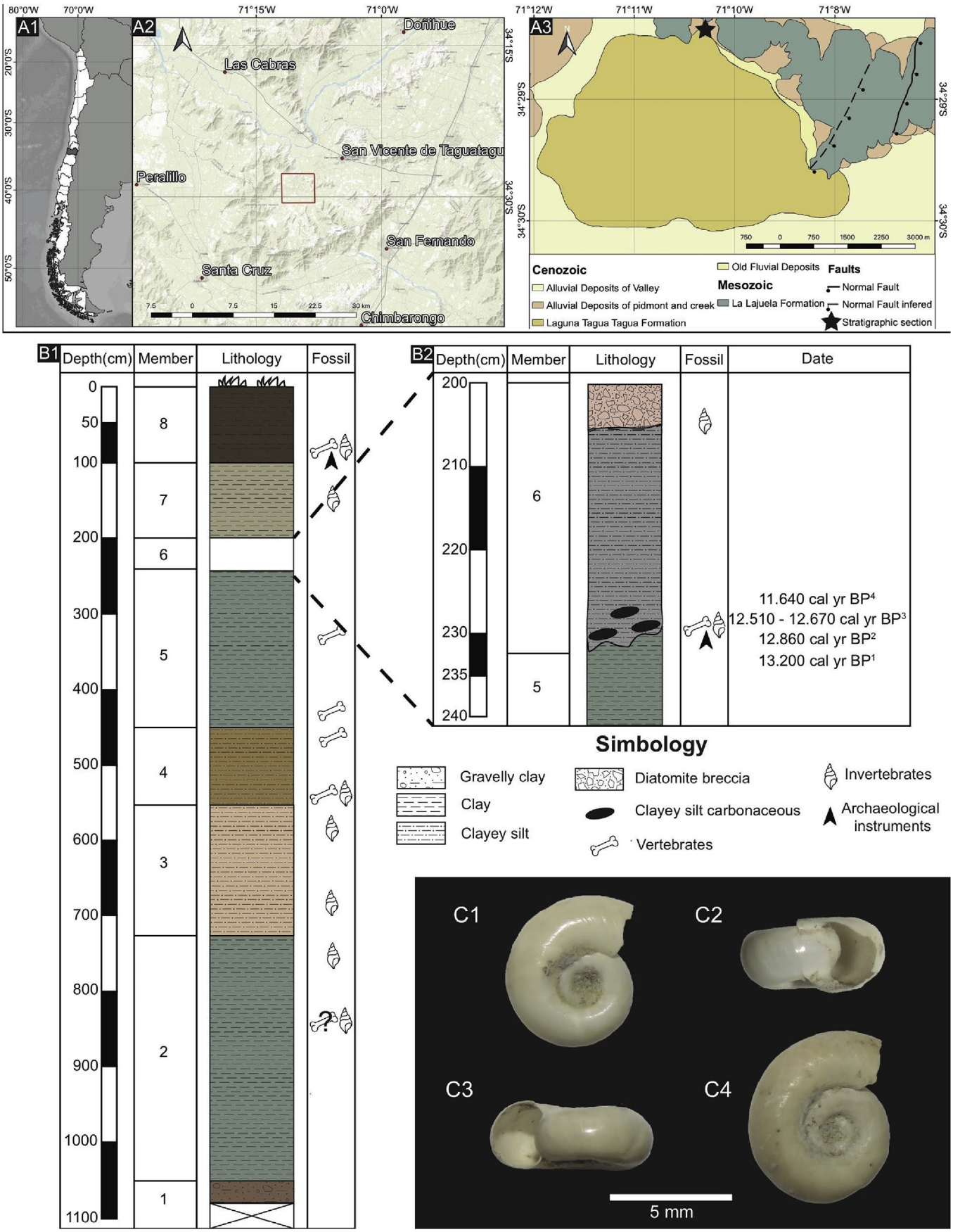

Fig. 1. Geographic location of the study area in South American (A1) and regional (A2) context. Geological setting of Laguna Tagua Tagua area (A3). Laguna de Tagua Tagua Formation (B1) and detail of the Pleistocene – Holocene transition (B2). Fossil remains of *Biomphalaria taguataguensis* from Taguatagua 1 SGO.PI.23,104 and SGO.PI.23,105 in lateral (C1, C4) and apertural (C2, C3) views. Scale bar = 5 mm. [1]Montané (1968); [2]Palma (1969); [3]This study; [4]Núñez et al. (1994).

9900 ± 100), both of them obtained from charcoal samples stratigraphically positioned at the lower section of member 6 and in stratigraphic association with lithic artefacts and megafauna bones. A third date, coming from right above the level of the human occupation at TT-2, gives a minimum age to this event of 11,000 cal yr BP (Beta-45518: 9710 ± 90).

In sum, the TT-1 archaeological occupation is a discrete event dated around ~12,600 cal yr BP, situated in a stratigraphic context deposited between ~13,590 and 11,070 cal yr BP. The bone assemblage analyzed here comes from this same stratigraphic context, allowing us to establish a late-Pleistocene to early-Holocene age for the assemblage. Further work, especially new excavations at the site with a detailed stratigraphic context and dating of the bone deposits are needed in the future.

2.3. Paleoenvironment and paleoclimate

During the late Pleistocene the climate of south-central Chile (~31°–42°S) was colder and more humid than today, and the environment was characterized by mesic C_3 vegetation (Kaiser et al., 2005, 2008). During the Last Glacial Maximum (LGM) (~26,000–19,000 cal yr BP), the amount of precipitation was double that of today (Moreno et al., 1999) and summer mean temperatures were between 6°C–8°C lower than today (Berman et al., 2016), which allowed the presence of large wooded areas. For example, at 32°S, swamp forests would have been occupying coastal areas (Villagrán and Varela, 1990) while, between 32° and 34°S, patches of deciduous and evergreen *Nothofagus* forests would have been present (Villagrán and Armesto, 1993). Between 34° and 36°S, in areas of low altitude, the environment was characterized by forests adapted to cold conditions and high precipitation values (Valero-Garcés et al., 2005), and/or by the presence of open mountain forests (Heusser, 1983). This high humidity levels have been related to the latitudinal displacement of the westerlies by at least 5° towards the equator (in conjunction with the Antarctic Circumpolar Current) (Kaiser et al., 2008). The Last Glacial Termination (~17,000–11,700 cal yr BP) in central Chile is characterized by a decrease in moisture, interrupted by one cold reversal event dated between 13,500–11,500 cal yr BP (Lamy et al., 1999; Valero-Garcés et al., 2005).

The early Holocene (~11,500–9,000 cal yr BP), between 31°S and 34°S, begins with an abrupt climate change towards more arid and warm conditions (Kaiser et al., 2008), reflected in a dramatic drop of arboreal taxa, with the concomitant expansion of grasslands such as Chenopodiaceae-Amaranthaceae (Heusser, 1983; Valero-Garcés et al., 2005). Geochemical and sedimentological evidence in LTT during the Pleistocene-Holocene transition shows an important lake level drop, which begins with the formation of the paleosoil that separates member 5 and member 6 (Varela, 1976). High and variable content of *Typha* also suggests the presence of a fluctuating large wetland surface (Valero-Garcés et al., 2005).

According to the chronology reported (Section 2.2), TT-1 is located at the end of the last LGT cold pulse, however the stratigraphic position of the site is more closely related to the Pleistocene-Holocene transition, and therefore with a passage from wet/cold to dry conditions.

2.4. Archaeology

TT-1 was archaeologically excavated during two field seasons (late 1960s and early 1990s), accounting for a total of around 189 m^2 of excavated area (Núñez et al., 1994; Montané, 1968). Casamiquela (1976) reported a taxonomic summary of the faunal remains coming from the first campaign, but no faunal data are published for the second one. Lithic tools and debitage, as well as bone tools were discovered spatially associated with fossils (Casamiquela, 1976; Núñez et al., 1994; Montané, 1968). The lithic assemblage is composed of a diversity of high-quality rocks, mainly aphanitic basalt and different siliceous rocks, but also includes obsidian (Méndez, 2015). Lithic tools were marginally retouched starting from big blanks and include bifacial knives, scrapers, side scrappers, and retouched flakes and blades. Use-wear analysis suggests cutting and scraping activities on soft and hard materials (Méndez, 2015). Debitage indicates in situ artifact preparation and/or maintenance. Montané (1968) also mentioned several bone tools made on horse bone, including flakers. No hearths were detected, but scattered charcoal spicules were found. In sum, all the evidence suggests a short-term camp in which mammal-processing activities were carried out (Méndez, 2015).

3. Materials and methods

Faunal remains come either from the top of the member 5 or the base of the member 6, covering a time span of ~2500 yr (see section 2.1 and 2.2). Fossils were identified using several reference neontological collections (Appendix A) and osteological guides (e.g. Barone, 1976; Baumel and Witmer, 1993; Cohen and Serjeantson, 1986; Falabella et al., 1995; Tercerie et al., 2016, among others). The taxonomic framework followed Dyer (1997) and Tercerie et al. (2016) for atherinopsines fishes, Frost et al. (2006) for anurans, Zaher et al. (2019) for colubrids, Prum et al. (2015), Gill and Donsker (2016), and Remsen et al. (2020) for birds, Mothé et al. (2017) for gomphotheres, Prado and Alberdi (2017) for equids, Alcaraz (2010) for extinct cervids and Patton et al. (2015) for rodents. For analytical purposes vertebrates were grouped into two categories according to its mass: small fauna (up to 10 kg) and megafauna (>44 kg). Small fauna includes rodents, marsupials, canids, birds, fishes, reptiles and anurans while megafauna incorporates gomphotheres, equids and cervids. Osteological terminology is based mainly on Gregory and Conrad (1937), Hershkovitz (1967), Lynch (1971), Barone (1976), Rage (1984), Baumel and Witmer (1993), Ferretti (2010), Gracian-Negrete et al. (2012), Gómez and Turazzini, 2016, among others. Measurements were taken with digital calipers to the nearest 0.01 mm. Eisenmann et al., 1988 measurement's guide for horses was used. Only for the third metatarsal of *Hippidion*, a Principal Component Analysis (PCA) was performed using the reference measurements from Prado and Alberdi (2017).

Due to the lack of information about the procedures of specimen collection during the excavation of TT-1, it is assumed the presence of a small fauna assemblage biased to larger taxa and/or larger specimens (Schaffer and Sánchez, 1994; Zohar and Belmaker, 2005). This caveat prevented detailed quantitative analysis. Only NISP (minimum number of specimens), MNI (minimum number of individuals) and NTAXA (number of identified taxa) were used for quantification (Grayson, 1984; Lyman, 2008). A specimen was considered "identified" when it was assigned at least to Class level.

Some general taphonomic attributes were recorded: weathering (Behrensmeyer, 1978), tooth marks (Binford, 1981), rodent marks (Lyman, 1994), digestive traces (Andrews, 1990; Fernández-Jalvo and Andrews, 1992), root marks (Fernández-Jalvo and Andrews, 2016), polishing/abrasion (Fernández-Jalvo and Andrews, 2003; Griffith et al., 2016), manganese coating (Marín-Arroyo et al., 2008, 2014), bioturbation (Pesquero et al., 2010), anthropic marks (e.g. cut marks, percussion marks, Mengoni-Goñalons, 1999) and thermal alterations (Shipman et al., 1984; Fernández-Jalvo et al., 2018). Fernandez-Jalvo and Andrews's modification atlas (2016) were used as reference. The specimens were inspected with low magnification lenses (up to 40×). A detailed taphonomic analysis is

in progress (Lizama-Catalán in prep.).

Due to manuscript length limitations, specimens identified at Order level or higher were not reported here. Only most significant or diagnostic fossils for each generic/specific taxon were presented. The specimens analyzed are housed in the Museo Nacional de Historia Natural of Santiago, Chile (MNHNCL) under the codes SGO.PV, SGO.PI. and TT. Repository codes of specimens described are listed in Appendix B.

All radiocarbon dates discussed in the text were calibrated to calendar years using the software Calib7.04 (Stuiver et al., 2019) and the SH13 calibration curve (Hogg et al., 2013).

4. Results

4.1. Systematic paleontology

4.1.1. Class Gastropoda Cuvier, 1795

4.1.1.1. Family Planorbidae Rafinesque, 1815

4.1.1.1.1. Genus Biomphalaria Preston, 1910

4.1.1.1.1.1. Biomphalaria taguataguensis Covacevich, 1971 (Fig. 1C, Table 1, Appendix B)

Mollusks from *Biomphalaria* are common in the assemblage analyzed. It corresponds to a small and thin discoidal-planispiral shell, with 2.5–3 convex whorls, whose width and height increase rapidly. The suture is well marked and deep. The shape of the aperture is semicircular; the width is similar to the height and the growth lines are thin, slightly marked and close to each other.

In comparative terms, the proportions of Aperture width/Maximum diameter and Aperture width/Umbilic diameter are notoriously greater in *B. taguataguensis* than in *B. chiliense* (Covacevich, 1971), which is observed in the specimens here described. Additionally, the chilean freshwater gastropods are characterized by a high degree of endemism according to the hydrological basin where they occur (Valdovinos, 2006), which makes biometric comparison with other taxa belonging to *Biomphalaria* difficult.

4.1.2. Class Actinopterygii Klein, 1885

4.1.2.1. Order Atheriniformes Bleeker, 1859

4.1.2.1.1. Family Atherinopsidae Fitzinger, 1873

4.1.2.1.1.1. Genus Odontesthes Evermann and Kendall, 1906

4.1.2.1.1.1.1. Odontesthes sp. (Fig. 2, Table 1, Appendix B)

Five specimens, including one right pre-opercular, two vomers and two quadrates belong to individuals of this genus (Fig. 2). The pre-opercular bone presents a spiny leaf, with a handsaw shape that widens in the medial zone. It also has a notorious central prominence with irregular edges and a curved angle >90°. In the lower portion, under the central prominence, it exhibits a sulcated slit that reaches the upper section. Thorny processes are absent. The fossils exhibit several features that permit its inclusion in the genus *Odontesthes*: a "L" shaped pre-operculum, a partially ossified sensory canal that runs through the bone at a straight angle, the vertical and partially closed branch with three pores, and pores 1 and 2 lacking a bone bridge as a separation (Dyer, 1997). Both vomer bones, identical in morphology, lack teeth in the anterior section (Dyer, 1997). The fossils are slightly concave ventrally, small, with an anterior articular section with two circular lateral condyles. In the middle of them, a triangular crest with a medial sulcus is present. The body is quadrangular in shape, with two dorsally pointed projections in the posterior section. The posterior process is projected from the middle of the body, which is thin and has a "sword blade" structure with striae in the form of "fullers" throughout it. The quadrate is a laminarly triangular plate, similar to an isosceles triangle, which begins in a wide articular condyle, forming a notorious articulation positioned in the anterior-proximal section. In proximal view, the joint has an inverted "T" shape. This condyle fits into the joint facet of the articular (angular) bone. A long process emerges from the articulation under the quadrate body which is projected posteriorly. Although similar in morphology, the quadrate articular heads in mugilids ends in several projections dorsally oriented (Froese and Pauly, 2019) not observed in the fossils from TT-1.

4.1.3. Clade Lissamphibia Haeckel, 1868

4.1.3.1. Order Anura Fischer von Waldheim, 1813

4.1.3.1.1. Family Calyptocephalellidae Reig, 1960

4.1.3.1.1.1. Genus Calyptocephalella Duméril and Bibron, 1841

4.1.3.1.1.1.1. Calyptocephalella gayi Dumèril and Bibron, 1841 (Fig. 3A–H, Table 1, Appendix B)

C. gayi is the most abundant taxon recovered in TT-1, with 840 identified specimens. Nearly half of the sample (48%) correspond to cranial elements.

Dermatocranium fossils show the typical exostosic ornamentation seen in *C. gayi*, with the presence of pits in immature individuals (Parker, 1881; Reinbach, 1939), bars in post-metamorphic individuals and tubercles in adults (Fig. 3A–C). Most of the specimens preserve its articulation plates (tonguelike process) that articulates with the nasal and squamosal. In ventral view, foramina for the entrance and exit of the occipital arteria, "Reinbach" channel and *lamina perpendicularis* are observed. Maxillae bones, which constitutes the orbital and temporal fenestra rim, are also well preserved. In the outer area of the *pars dentalis*, an almost complete dentition (excepting the posterior area) along the maxillae is observed, a typical trait of *C. gayi*. The sphenoid is anteriorly expanded, starting from the nasal capsule to the anterior border of the orbit in its most posterior portion. In dorsal view exhibits a "V-shaped" notch for the frontoparietal joint which is separated by a keel. In ventral view it is possible to observe the marks left by the parasphenoid in the anterolateral border (Muzzopappa et al., 2016).

Although less represented, bones of the scapular girdle are present in the assemblage. Some scapulae preserve a crest or *tenuitas cristaeformi* located in the anterior border, which is diagnostic of *C. gayi* (Muzzopappa et al., 2016) (Fig. 3F). Pelvic girdle fossils also represent different ontogenetic stages, with the ilion as one of the most diagnostic bones among the anurans (Bever, 2005; Gómez and Tuzzarini, 2015). In the ilion analyzed, the iliac ramus presents a high dorsal crest, which expands from the base of the dorsal prominence to almost two-thirds of the anterior axis. The dorsal tubercle is high and its border is located near to the terminal rim of the acetabulum (Muzzopappa et al., 2016). Finally, the acetabular rim is high and limits with the pre-acetabular area, which possesses a near 90° angle with respect to the iliac ramus (Fig. 3H).

Regarding limb bones, humeri, radius-ulna, femora, tibia-fibula, tibiae, and fibulae were identified. Among these, the humerus is particularly diagnostic of the species. The distal epiphysis presents a marked lateral and medial expansion of its ulnar and radial epicondyles, and a humeral sphere which possess a diameter that exceeds the half of its distal breath. The humeral sphere is also laterally displaced from the longitudinal axis of the diaphysis (Muzzopappa et al., 2016; Otero et al., 2014; Suazo-Lara et al., 2017, 2018). The humerus is more robust than other anuran species and possesses a well-developed deltoid crest. In spite of the fact that this feature has been reported also in *Telmatobius* sp., the humerus in the species of this genus exhibits a big lateral crest and prominence in the proximal border of the deltoid crest, which is not observed in the specimens analyzed (Suazo-Lara et al., 2018)

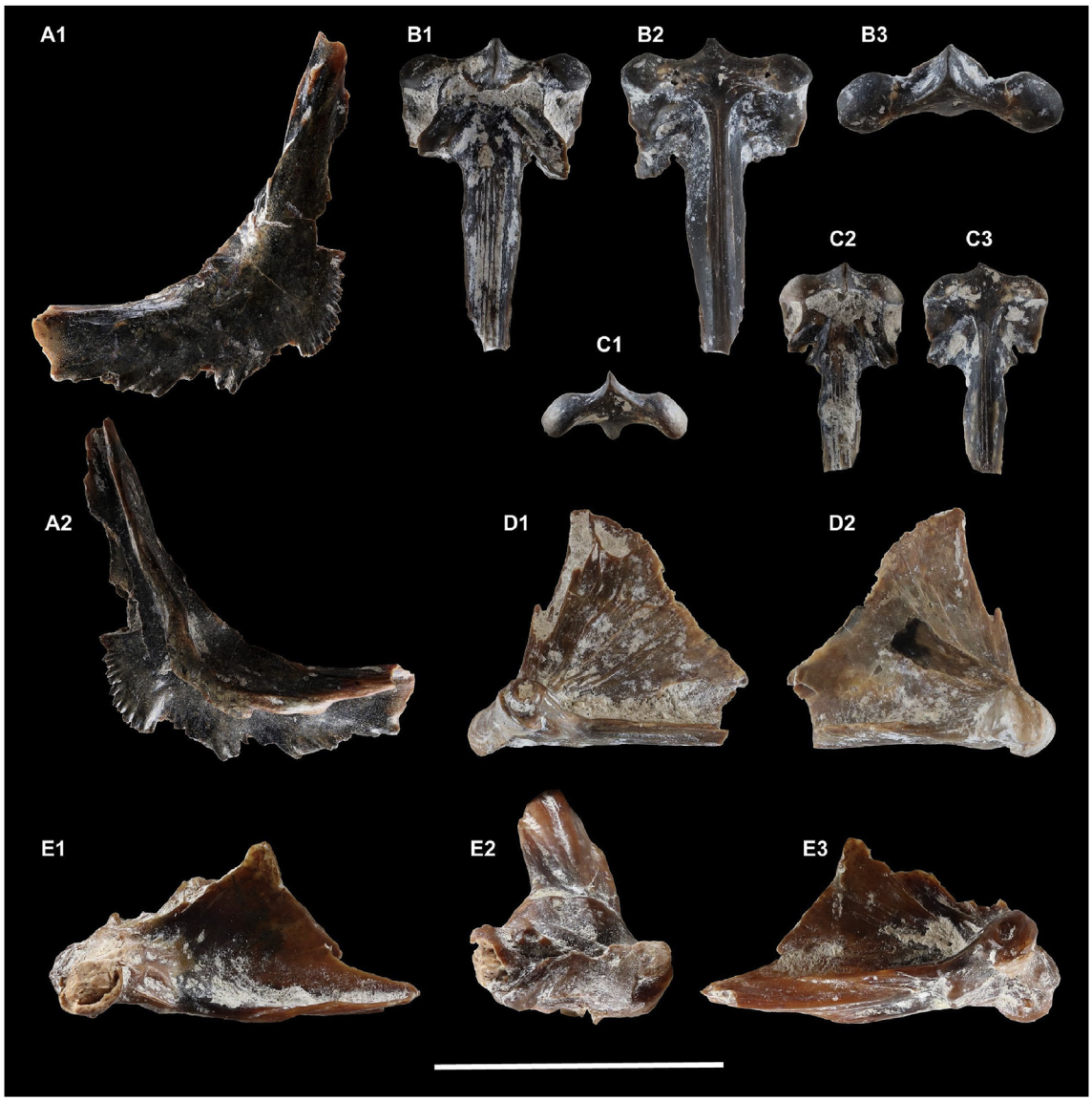

Fig. 2. Remains of *Odontesthes* sp. from Taguatagua 1 site. Left preoperculum fragment SGO.PV.25,165 in lateral external (A1) and lateral internal (A2) views. Vomer fragment SGO.PV.24,782-e in dorsal (B1), ventral (B2) and frontal (B3) views. Vomer fragment SGO.PV.24,782-f in dorsal (C1), ventral (C2) and frontal (C3) views. Quadrate fragment SGO.PV.24,782-d in lateral internal (D1) and lateral external (D2) views. Quadrate fragment SGO.PV.25,280-b in lateral internal (E1), frontal (E2) and lateral external (E3) views. Scale bars: A1-A2 = 20 mm, B1-E3 = 10 mm.

(Fig. 3G). A total of 92 individuals were estimated to be present in the assemblage. The sample includes both cranial and postcranial bones at different ontogenetic stages (larvae, juvenile, and adult) following Gosner (1960). The age profiles suggest mainly larvae individuals (%MNI = 67,4), and fewer juveniles (%MNI = 17,4) and adults (%MNI = 15,2).

4.1.3.1.2. Family Bufonidae Gray, 1825

4.1.3.1.2.1. Genus Rhinella Fitzinger, 1826

4.1.3.1.2.1.1. Rhinella sp. (Fig. 3I, Table 1, Appendix B)

Only one complete scapula from an adult individual was identified (MNI = 1). The specimen is almost indistinguishable from the extant *Rhinella spinulosa* and *Rhinella arunco* reference specimens. The elements of the scapular girdle lack diagnostic features among the Bufonidae, nevertheless the spinulosa group presents a short and wide scapula (Tihen, 1962) and lacks an anterior lamina, anteriorly projected, a trait that is observed in Calyptocephalellidae.

4.1.4. Class Reptilia Laurenti, 1768

4.1.4.1. Order Squamata Oppel, 1811

4.1.4.1.1. Family Dipsadidae Bonaparte, 1838

4.1.4.1.1.1. Genus Philodryas Wagler, 1830

4.1.4.1.1.1.1. cf. Philodryas sp. (Fig. 3J-L, Table 1, Appendix B)

The studied material includes three pre-cloacal vertebrae and one caudal vertebra (Fig. 3J-L). All the specimens have strong procoely in the centrum, with circular articular faces in the cotyla and condyle. The neural arch is laterally expanded and the zygapophyses are horizontal. The neurapophysis is broken in all specimens, although the base can be observed, which is thin and reaches the zygantrum. There are lateral and paracotylar foramina in the centrum. In the pre-cloacal vertebrae, the diapophysis and parapophysis are located in the anteroventral border of the centrum,

Fig. 3. Selected anurans and reptiles remains from Taguatagua 1 site. *Callyptocephalella gayi*, cranial and postcranial remains (A–H). Frontoparietals from different ontogenetical stages; SGO.PV.24,218 in dorsal (A1) and ventral (A2) views; SGO.PV.26,469 in dorsal (B1) and ventral (B2) views and SGO.PV.24,369 in dorsal (C1) and ventral (C2) views. Dorsal vertebra VI SGO.PV.24,190-a in anterior (D1) dorsal (D2) and posterior (D3) views. Dorsal vertebra II SGO.PV.24,190-b in posterior (E1) and dorsal (E2) views. Left scapula SGO.PV.24,191 in dorsal (F1) and ventral (F2) views. Left humerus SGO.PV.23,923 in anterior (G1), medial (G2), posterior (G3) and lateral (G4) views. Right ilium SGO.PV.23,945 in lateral (H1) and dorsal (H2) views. *Rhinella* sp., right scapula SGO.PV.20,638 in dorsal (I1) and ventral (I2) views. cf. *Philodryas* sp. axial remains (J–L). Precloacal vertebra SGO.PV.25,221 in anterior (J1), dorsal (J2), posterior (J3), left lateral (J4) and ventral (J5) views. Precloacal vertebra SGO.PV.26,019 in anterior (K1), dorsal (K2), posterior (K3), right lateral (K4) and ventral (K5) views. Caudal vertebra SGO.PV.25,222 in anterior (L1), dorsal (L2), posterior (L3), left lateral (L4) and ventral (L5) views. Scale bars: A1-H2 = 40 mm; I1, I2 = 20 mm; J1-L5 = 10 mm.

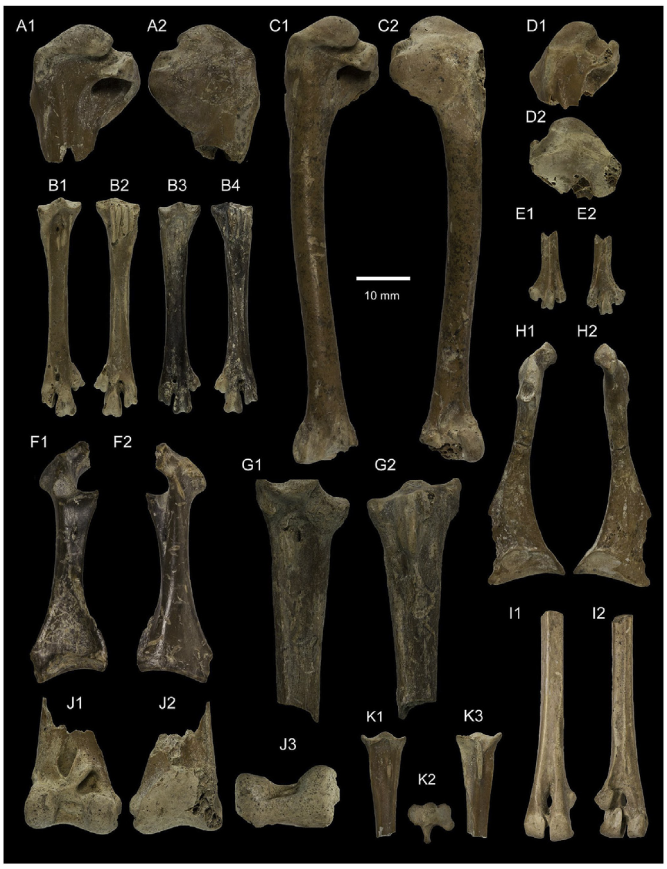

Fig. 4. Birds remains from Taguatagua 1 site. cf. *Lophonetta specularioides*, left proximal humerus SGO.PV.23,279 in caudal (A1) and cranial (A2) views. *Anas* cf. *A. flavirostris*, right tarsometatarsus SGO.PV.26,347 in dorsal (B1) and plantar (B2) views and SGO.PV.26,348 in dorsal (B3) and plantar (B4) views. *Anas* cf. *A. georgica*, left humerus SGO.PV.26,350 in caudal (C1) and cranial (C2) views. Columbidae indet., left proximal humerus SGO.PV.20,203 in caudal (D1) and cranial (D2) views. *Zenaida* sp., left distal tarsometatarsus SGO.PV.26,353 in cranial (E1) and plantar (E2) views. *Fulica* cf. *F. rufifrons*, left coracoid SGO.PV. 20181 in dorsal (F1) and ventral (F2) views. *Fulica* cf. *F. armillata*, right proximal tarsometatarsus SGO.PV.20,182 in dorsal (G1) and plantar (G2) views. *Podiceps major*, left coracoid SGO.PV.23,227 in dorsal (H1) and ventral (H2) views and right tarsometatarsus SGO.PV.20,166 in dorsal (I1) and plantar (I2) views. *Geranoaetus melanoleucus*, right distal tibiotarsus SGO.PV.26,354 in cranial (J1), caudal (J2) and distal (J3) views. *Milvago* cf. *M. chimango*, right proximal tarsometatarsus SGO.PV.23,203 in dorsal (K1), proximal (K2) and plantar (K3) views. Scale bar = 10 mm.

being the parapophysis anteriorly displaced respect to the diapophysis (Fig. 3J and K). The haemal keel extends along the entire length of the centrum. The combination of strong procoely in the vertebral centrum, haemal keel, expanded neural arches and presence of zygosphene-zygantrum articulation in the latter are typical characters of ophidians (Rage, 1984). The specimens also present an elongated vertebral centrum in a cranio-caudal sense, a well-developed condyle with circular shape in articular view, subhorizontal zygapophyses and well developed prezygapophyseal processes, which are typical traits of the clade Colubroides (Holman, 2000; Rage, 1984). The absence of a well-developed hypapophysis in the precloacal vertebrae allows to discard the assignment of the specimens to the families Elapidae and Viperidae (Albino, 1989; Rage, 1984) and suggests that these may belong to a 'colubrid' grade snake. The fossil material from TT-1 shares some features with *Philodryas chamissonis,* but no with *Tachymenis chilensis*, such as a higher neural arch (including an oval neural canal in articular view), a craniocaudally shorter neural spine, and the presence of a bigger prezygapophyseal process which are anterolaterally oriented. Due to the difficulty for making a more extensive comparison with the vast diversity of colubroides and the complicated taxonomy which is in constant flux (Grazziotin et al., 2012; Zaher et al., 2009, 2019) the fossils are conferred tentatively to *Philodryas* genus. MNI = 1 is estimated.

4.1.5. Class Aves Linnaeus, 1758

4.1.5.1. Order Anseriformes Wagler, 1830

4.1.5.1.1. Family Anatidae Leach, 1819

4.1.5.1.1.1. Genus Lophonetta Riley, 1914

4.1.5.1.1.1.1. cf. Lophonetta specularioides King, 1828 (Fig. 4A, Table 1, Appendix B)

So far, only two proximal humerus portions have been identified for this taxon. Among the shared features between both fossil fragments and the humerus of *Lophonetta specularioides* are: a deep, rounded and mediocaudally oriented *fossa pneumotricipitalis ventralis*, which in its interior has multiple foramina, a feature that is common in anatids (Worthy, 2004); the *tuberculum centrale* is robust and acute proximally and wide distally; the *crus dorsale* is well marked; the *incisura capitis* is deep, short and wide, as in other members of Anatinae (Tonni, 1969; Woolfenden, 1961), and it is partially covered by the caudal end of the *caput humeri*. In both fossil and reference specimens, the *caput humeri* is rounded and well developed and the *sulcus ligamentous transversus* is broad proximodistally and slightly extended dorsoventrally. The *fossa pneumotricipitalis dorsalis* is excavated below the humeral head, which is a feature that has been observed in *Lophonetta* genus (De Mendoza and Tambussi, 2019). Additionally, the *capital groove* is mediocaudally oriented and the *tuberculum dorsale* is reduced and elongated, which are also features described in *Lophonetta* (Campbell, 1973). Although there is high osteological homogeneity within Anatidae family (Zelenkov, 2010; Zelenkov and Kurochkin, 2012), the morphology and proportions of the fossil specimens are practically indistinguishable from *L. specularioides* but different to other anatines (e.g. *Anas flavirostris*, *Anas georgica*, *Anas platyrhynchos*, *Oxyura* spp.). Due to this, the remains are tentatively conferred to *Lophonetta specularioides*. MNI = 1 is estimated.

4.1.5.1.1.2. Genus Anas Linnaeus, 1758

4.1.5.1.1.2.1. Anas cf. A. flavirostris Vieillot, 1816 (Fig. 4B, Table 1, Appendix B)

Three specimens are assigned to this taxon, including two complete right tarsometatarsi and a proximal half of a right tarsometatarsus. The fossils present a *fossa infracotylaris dorsalis* slightly excavated, which is a typical feature of the Anatidae (Cohen and Serjeantson, 1986; Gilbert et al., 1981), with a central foramen proportionally large as it is observed in *Anas flavirostris*. As in *Anas flavirostris*, the specimens have two *tuberositas musculi tibialis cranialis*, longitudinally elongated and parallel to each other, of which the medial is located more proximally than the lateral. The *cotyla medialis* is markedly concave and more proximally projected than the *cotyla lateralis*; the diaphysis has a nearly quadrangular section as is described in Anatidae (Worthy et al., 2007); the *foramen vasculare distale* is proportionally large and ellipsoidal in shape, with its longitudinal axis larger than the transversal one; the *trochlea metatarsi II* is inclined plantarly, and it is more proximally positioned than the *trochlea metatarsi IV*, not surpassing in extension to the *incisura intertrochlearis medialis*, which is between the *trochlea metatarsi II* and the *trochlea metatarsi IV*. These traits of the trochlea are typical of the diver anatids (Worthy et al., 2007). The *trochlea metatarsi II* has a prominent groove, which is a feature described in Anatinae (Woolfender, 1960). In proximo-plantar view, four well-defined *cristas hypotarsi* are observed, which in turn, generates three *sulci*. This morphology is also typical among Anatidae (Cohen and Serjeantson, 1986; De Mendoza and Tambussi,

2019; Gilbert et al., 1981). As in *Anas flavirostris*, the medial and intermediate sulcus are partially closed, while the lateral sulcus is open. Additionally, the length and proportions of the tarsometatarsi is similar to the *Anas flavirostris* reference specimen, but different from the tarsometatarsus of *Lophonetta specularioides* and *Anas georgica*.

The fossils are referred to *Anas* cf. *A. flavirostris* considering their indistinguishable morphology and proportions from those of the reference specimens MNI = 3 is estimated.

4.1.5.1.1.2.2. Anas cf. A. georgica Gmelin, 1789 (Fig. 4C, Table 1, Appendix B)

Three humeri, one of them complete, are conferred to this taxon. All the fossils exhibit a straight *crista deltopectoralis*, with a dorsal orientation and a short and wide incisura capitis. In addition, the ventral portion of the *fossa pneumotricipitalis* presents a large *foramen pneumaticum*, composed of many foramina that communicate towards the interior of the bone. These traits permit their inclusion in the genus *Anas* (Tonni, 1969; Woolfenden, 1961; Worthy, 2004). Among the similarities observed between the humerus of reference specimens of *Anas georgica* and fossil materials are their proportions and the *tuberculum ventrale*, which is proximodistally elongated, unlike *Lophonetta specularioides* in which is more robust. Also, the morphology of the *margo caudalis* is identical to *Anas georgica*, but is less marked than in *L. specularioides*, giving to the diaphysis a more rounded surface. Unlike *Anas flavirostris*, the fossil humerus has a marked groove on the ventral surface of the *tuberculum ventrale*. In addition, the *tuberculum dorsale* in the humerus of *A. flavirostris* is rounded at its distal edge, while it is acute in the fossil specimen. Also, the *fossa musculi brachialis* extends less proximally in the fossil humerus than in the *A. flavirostris* humerus. The almost indistinguishable morphology between the fossil materials and the reference material allow us to confer them to *Anas* cf. *A. georgica*. MNI = 2 is estimated.

4.1.5.2. Order Podicipediformes Fürbringer, 1888

4.1.5.2.1. Family Podicipedidae Bonaparte, 1831

4.1.5.2.1.1. Genus Podiceps Latham, 1787

4.1.5.2.1.1.1. Podiceps major Boddaert, 1783 (Fig. 4H and I, Table 1, Appendix B)

An incomplete right tarsometatarsus and a left coracoid are identified as belonging to great grebes. The hypotarsus exhibits three bony channels that form a "V". Two of them are small and the third is comparatively larger and located in the middle of this feature, although slightly displaced dorsomedially. This particular arrangement is diagnostic of Podicipediformes (Gilbert et al., 1981). On the other hand, the *crista medialis hipotarsi* and the *crista lateralis hipotarsi* are markedly projected and delimit a deep *sulcus hipotarsi*, a feature also diagnostic of the Podicipedidae (Mayr, 2004). The *foramen vasculare distale* is proportionally large and the facets of the trochlea in cranial view do not present grooves but are rounded, which are diagnostic features of the order Podicipediformes (Gilbert et al., 1981). Finally, one of the specimens preserves part of the diaphysis, which is mediolaterally compressed and is rhomboidal in cross section, which is typical in Podicipedidae (Chéneval and Escuillié, 1992).

Among the diagnostic features in the coracoid of the Podicipediformes are the absence of a *procoracoid processus* and the rounded shape of the diaphysis in the area that constitutes the trioseus channel (Gilbert et al., 1981). Both in the coracoid of reference specimens of *Podiceps major* and in the fossil specimen, the surface of the *facies articularis sternalis* expands both to the dorsal (in which it has a semicircular shape) and ventral surface (in which the highest edge it is located medially), giving to the coracoid a structure that is inserted into the *sulcus articularis coracoideus* of the sternum, which has a pocket-shape (Baumel and Witmer, 1993).

Both, the coracoid and the tarsometatarsus, have the same size as the reference specimen of *Podiceps major*, which is the largest extant grebe present in Chile reaching a maximum length between 70 and 78 cm (Jaramillo, 2005). MNI = 1 is estimated.

4.1.5.3. Order Columbiformes Latham, 1790

4.1.5.3.1. Family Columbidae, Illiger 1811

4.1.5.3.1.1. Genus Zenaida Bonaparte, 1838

4.1.5.3.1.1.1. Zenaida sp. (Fig. 4E, Table 1, Appendix B)

A distal tarsometatarsus is assigned to this taxon. It can be grouped within the Columbidae based on the presence of a broad and well-marked *fossa metatarsi* I that surpasses the medial border of the *facies dorsalis,* and the marked medial inflection of the *trochlea metatarsi* II (Worthy and Wragg, 2008). As in the tarsometatarsus of *Zenaida meloda* and *Zenaida auriculata*, in the plantar surface of the fossil fragment, the terminal section of the *crista medialis* is observed, which flanks the medial edge of the *fossa metatarsi* I. Although the proportions and morphology are similar to those observed in *Zenaida meloda*, the morphology of this element also resembles that observed in *Zenaida auriculata*. Based on the morphological similarity with the comparative specimens, the fossil is referred to *Zenaida* sp. MNI = 1 is estimated.

4.1.5.3.1.1.2. Columbidae indet. (Fig. 4D, Table 1, Appendix B)

A proximal fragment of a left humerus is referred to an undetermined Columbiformes. The fossil has a deep and wide capital groove and a prominent deltoid crest, typical features of Columbiformes (Cohen and Serjeantson, 1986). Among the characteristics of Columbidae present in the fossil are: a *caput humeri* markedly convex proximally; a *tuberculum dorsale* elongated and merged with the *caput humeri* medially; a *fossa pneumotricipitalis* very pneumatic, large, rounded and caudally oriented. Also, the *crista deltopectoralis* is marked and short, approximately triangular and oriented anterodorsally, and the *impressio coracobrachialis* is poorly marked (Cohen and Serjeantson, 1986; Worthy and Wragg, 2008).

According to its size, the specimen belongs to a columbiform larger than the species *Zenaida auriculata, Zenaida meloda, Columbina cruziana, Metropelia aymara* and *Columba livia* used as reference specimens. This difference in size suggests that the element could belong to the genus *Patagioenas*, since it is the largest columbiform currently present in Chile (Couve et al., 2016; Martínez-Piña and González-Cifuentes, 2017). MNI = 1 is estimated.

4.1.5.4. Order Gruiformes Bonaparte, 1854

4.1.5.4.1. Family Rallidae Rafinesque, 1815

4.1.5.4.1.1. Genus Fulica Linnaeus, 1758

4.1.5.4.1.1.1. Fulica cf. F. rufifrons Philippi and Landbeck, 1861 (Fig. 4F, Table 1, Appendix B)

The sample includes only one coracoid. It presents a *tuberculum brachiale* not undercut, a pronounced *processus procoracoideus* which extends further medially than the *processus acrocoracoideus*, a large and deep *cotyla scapularis*, a *facies articularis humeralis* rounded, about as wide as long, which flares strongly laterally, and an *impressio musculi sternocoracoidei* deep and very anteriorly extended. These are diagnostic traits of the family Rallidae (Boles, 2005). The morphology of the fossil coracoid is similar to those observed in *Fulica rufifrons*, since the coracoid in this species has a narrower diaphysis than both *Fulica leucoptera* and *Fulica armillata*, and an *extremitas omalis* smaller than *F. armillata* and *Fulica leucoptera*. In medial view, the *processus acrocoracoideus* has a straight proximal edge of the *facies articularis clavicularis*, which is convex in *F. leucoptera* and *F. armillata*. In addition, the *tuberculum brachiale*

is very little developed and, in lateral view, the *cotyla scapularis* is slightly excavated, in contrast to *F. leucoptera* and *F. armillata*, in which it is deeply excavated (Cenizo et al., 2015). MNI = 1 is estimated.4.1.5.4.1.1.2. *Fulica* cf. *F. armillata* Vieillot 1817 (Fig. 4G, Table 1, Appendix B)

One right metatarsus of the Red gartered coot was identified. In proximal view, the hypotarsus has an elongated triangular shape. In plantar view, two *sulci hypotarsi* are observed and the *crista lateralis hypotarsi* is prominent and is extended distally. All the features are diagnostic of the family Rallidae (Boles, 2005). Also, the fossil exhibits a large and distinct *tuberositas musculi tibialis cranialis*, which shows a flat dorsal surface, a common feature of the genus *Fulica*. The almost indistinguishable morphology between the fossil and the tarsometatarsus of the reference specimens of red gartered coot suggests its inclusion in this species. MNI = 1 is estimated.

4.1.5.5. Order Accipitriformes Vieillot, 1816
4.1.5.5.1. Family Accipitridae Vigors, 1824
4.1.5.5.1.1. Genus Geranoaetus Kaup, 1844
4.1.5.5.1.1.1. Geranoaetus melanoleucus Vieillot, 1819 (Fig. 4J, Table 1, Appendix B)

The sample is composed only by a distal end of a right tibiotarsus. As with most accipitrids, this bone is craniocaudally narrow (Manegold et al., 2014). Both in the fossil and the reference specimen of black-chested buzzard-eagle, the *pons supratendineus* is robust and is oriented diagonally with respect to the longitudinal axis of the element, as in other accipitrids (Manegold et al., 2014). The *sulcus extensorius* deepens distally and continues with the *canalis extensorius*, which is arranged medially with respect to the former. The *sulcus intercondylaris* is well marked and broad mediolaterally. The distal border of the *condylus medialis* is slightly more distally extended than the *condylus lateralis*. Additionally, the size and proportions are comparable to those of the tibiotarsus of *Geranoaetus melanoleucus*, but different respect to the *Geranoaetus polyosoma* and *Parabuteo unicinctus* used as a reference. MNI = 1 is estimated.

4.1.5.6. Order Falconiformes Sharpe, 1874
4.1.5.6.1. Family Falconidae Leach, 1820
4.1.5.6.1.1. Genus Milvago Spix, 1824
4.1.5.6.1.1.1. Milvago cf. M. chimango Vieillot, 1816 (Fig. 4K, Table 1, Appendix B)

So far, only a proximal fragment of right tarsometatarsus assigned to this taxon is identified. The bone is referred to the Falconidae according to the presence of a *crista medialis hypotarsi*, straight and well developed, which continues distally on the medial aspect of the diaphysis as a *crista medialis planaris*. In Accipitridae this feature is less marked and more medially located (Cenizo and Tassara, 2013; Noriega et al., 2011). Additionally, the *tuberositas musculi tibialis cranialis* is not well developed, the *crista lateralis hipotarsi* is reduced and the *fossa parahypotarsalis medialis* (the area where the *musculi flexor hallucis brevis* is inserted) is confined to the medial surface of the tarsometatarsus, whereas in Accipitridae it is more centrally located (Cenizo and Tassara, 2013). In addition, the fossil presents several features that are indistinguishable from those present in the tarsometatarsus of the falconid *Milvago chimango*: the *tuberositas m. t. cranialis* is relatively short and is located near the medial edge of the diaphysis; the *fossa infracotylaris dorsalis* is very broad and well excavated, covering most of the diaphysis; the *sulcus extensorius* is marked and extends distally; both the *cotyla medialis* and the *cotyla lateralis* have concave articular surfaces and are separated by a prominent and round *eminentia intercotylaris* and the *crista lateralis hypotarsi* is dorsoventrally flattened and latero-caudally oriented. MNI = 1 is estimated.

4.1.6. Class Mammalia Linnaeus, 1758
4.1.6.1. Infraclass Marsupialia Illiger, 1811
4.1.6.1.1. Order Didelphimorphia Gill, 1982
4.1.6.1.1.1. Family Didelphidae Gray, 1821
4.1.6.1.1.1.1. Genus Thylamys Gray, 1843
4.2.6.1.1.1.1.1. Thylamys sp. (Fig. 5A, Table 1, Appendix B)

A single mandibular fragment is assigned to this marsupial. In this specimen, the horizontal ramus or dentary is anteroposteriorly elongated with an inflected lower border, as graceful as observed on *Thylamys*. The coronoid process and the mandibular condyle are incomplete, and the retromolar space is imperforate, notorious and larger than observed in didelphini members such as *Chironectes, Didelphis, Metachirus* and *Philander*. The masseteric fossa is well developed, more pronounced and acuminate than observed in *Marmosa* and *Marmosops*, and more acuminate anteriorly than *Monodelphis*. The angular process is broken, but it was probably projected straight towards medial. No mental foramina are preserved. The m3 and m4 are compressed labio-lingually, with a talonid higher than the trigonid, and are almost identical in its antero-posterior length. The hypoconid of the m3 is labially salient,

Fig. 5. Marsupial and selected rodents remains from Taguatagua 1 site. *Thylamys* sp., right mandible SGO.PV.22,252 in lateral (A1) and medial (A2) views. *Myocastor coypus*, cranial and postcranial remains (B–D). Right p4 SGO.PV.2003-C in occlusal (B1) and posterior (B2) views. Left calcaneus SGO.PV.25,626 in plantar (C1) and medial (C2) views. Right tibia SGO.PV.25,628 in medial (D1) and caudal (D2) views. *Octodon degus*, cranial remains (E–F). Left maxilla SGO.PV.20,109 in lateral (E1), medial (E2) and occlusal (E3) views. Right mandible SGO.PV.20,122 in lateral (F1), medial (F2) and occlusal (F3) views. *Octodon bridgesii*, cranial remains (G–H). Left dentary SGO.PV.25,531 in lateral (G1), medial (G2) and oclusal (G3) views. Right M1 SGO.PV.20,119 in occlusal (H1) and palatal (H2) views. *Octodon* cf. *O. lunatus*, left mandible SGO.PV.25,641 in lateral (I1), medial (I2) and occlusal (I3) views. *Spalacopus cyanus*, right mandible SGO.PV.20,121 in medial (J1), lateral (J2) and occlusal (J3) views. *Aconaemys fuscus*, left mandible SGO.PV.2015 in lateral (K1), medial (K2) and occlusal (K3) views. *Abrocoma bennettii*, left mandible SGO.PV.25,637 in lateral (L1), medial (L2) and occlusal (L3) views. Scale bars: A1, A2 and H1, H2 = 5 mm. C1, C2 = 20 mm. D1, D2 = 30 mm. B1, B2, E1- G3, I1 – L3 = 10 mm.

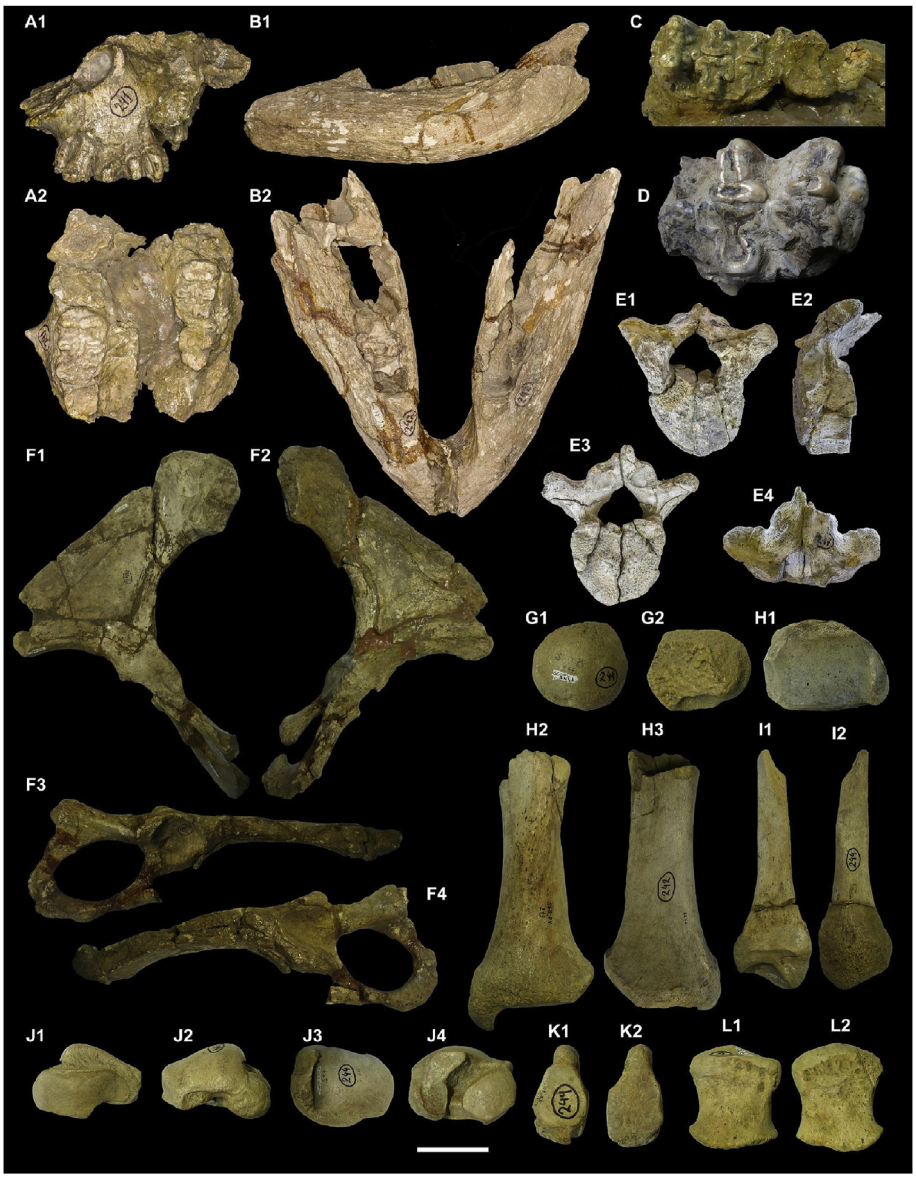

Fig. 6. Gomphotheriidae indet. remains from Taguatagua 1 site. Maxillary fragment SGO.PV.241 in left lateral (A1) and caudal (A2) views. Mandible SGO.PV.242-b in left lateral (B1) and cranial (B2) views. Detail of right P4-M1 SGO.PV.241, in occlusal view (C). M1 SGO.PV.26,520 in occlusal view (D). Thoracic vertebrae SGO.PV.247 in cranial (E1), lateral (E2), caudal (E3) and dorsal (E4) views. Left and right pelvis SGO.PV.243-a and b in caudal (F1–F2) and lateral (F3–F4) views. Unfused femoral head SGO.PV.244-b in proximal and distal views. Left distal tibia in distal (H1), cranial (H2) and caudal (H3) views. Left distal fibula SGO.PV.244-a in medial (I1) and lateral views (I2). Left astragalus SGO.PV.244-e in dorso-distal (J1), ventro-proximal (J2), proximal (J3) and distal (J4) views. Tarsal sesamoid SGO.PV.244-c in dorsal (K1) and plantar (K2) views. Unfused fourth? metatarsal SGO.PV.244-d in dorsal (L1) and plantar (L2) views. Scale bar for A1-B2, E1-E4 and G1-J4 = 10 cm. Scale bar for C, D and K1-L2 = 5 cm. Scale bar for F1–F4 = 20 cm.

like in most opossums. The entoconid of the m3 is well developed compared with the hypoconid, and larger than the hypoconulid. Both m3 and m4 fossil material are equal in size and morphology compared with the extant *T. elegans* reference specimen. The m2 alveolus suggests a similar size between the m2 and m3. The SGO.PV.22,252 feature set allows to assign the material to didelphidae genus *Thylamys*, but more diagnostic features are necessary to get a specific assignment. MNI = 1 is estimated.

4.1.6.2. Infraclass Placentalia Owen, 1837

4.1.6.2.1. Order Proboscidea Illiger, 1881

4.1.6.2.1.1. Family Gomphotheriidae Cabrera, 1929

4.1.6.2.1.1.1. Gomphotheriidae indet (Fig. 6, Table 1, Appendix B)

Nineteen proboscidean fossils were recovered, including six molar fragments, three cranial fragments, a mandible, both pelvis, a thoracic vertebra, a femoral head, a distal right tibia, a distal right fibula, a right astragalus, a metatarsal IV? and a tarsal sesamoid. The wearing stages observed in the maxillar with its left and right P4 very worn, without any figure and both M1 with advanced wear in first and second lophs (Fig. 6C), suggests an age-at-death of 12,5–22 years according to Mothé et al. (2010). A second individual, probably a young individual, is represented by an isolated fragmented M1 (Fig. 6D). The mandible, without teeth, has a portion of the m3 alveolus above the ramus, which suggest that this dental piece may not have completely erupted (Fig. 6B). Considering the sexual dimorphism indicated for the family Gomphotheriidae (Labarca, 2020; Mothé et al., 2010), the distal transvrse diameter of the tibia suggests that it belonged to a male (Fig. 6H). All the distal tibia, distal fibula, and astragalus articulate with each other, but the relation with the cranial fragments is not clear (Fig. 6H-J). The

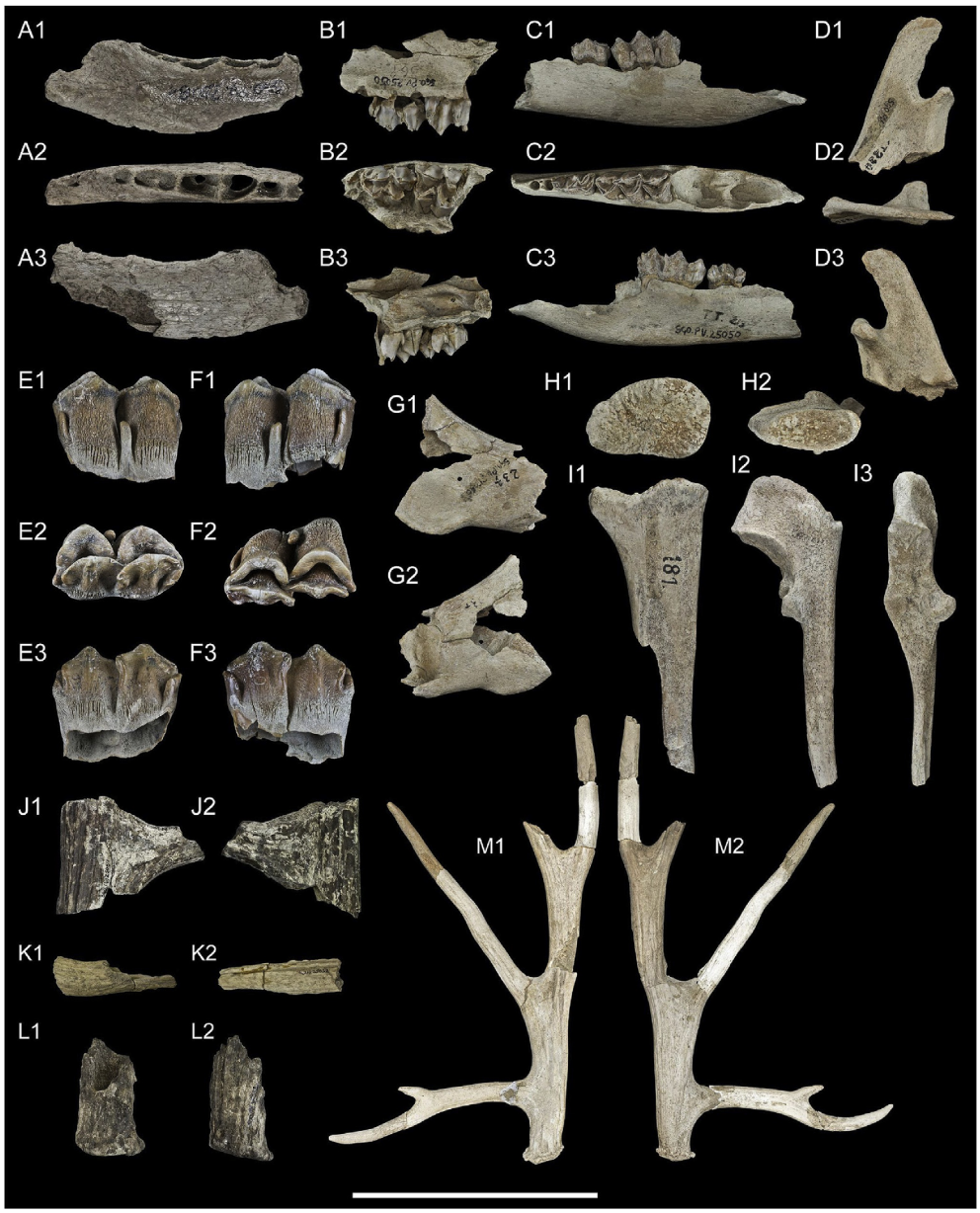

Fig. 7. Canids and Cervids remains from Taguatagua 1 site. *Lycalopex culpaeus*, right dentary fragment SGO.PV.25,081 in labial (A1), occlusal (A2) and lingual (A3) views. Cervidae indet., cranial and postcranial remains (B–F). Left maxilla SGO.PV.25,050–1 in labial (B1), occlusal (B2), lingual (B3) views. Left dentary fragment SGO.PV.25,050–5 in labial (C1), occlusal (C2) and lingual (C3) views. Left coronoid process SGO.PV.25,050–7 in labial (D1), dorsal (D2) and lingual (D3) views. Left SGO.PV.25,050–4 and right SGO.PV.25,050-2-3 m1 in labial (E1, F1), occlusal (E2, F2) and lingual (E3, F3) views respectively. Right dentary fragment SGO.PV.25,050–6 in labial (G1) and lingual (G2) views. Proximal left radius SGO.PV. 25050–8 in cranial (H1) and posterior (H2) views. Proximal left ulna SGO.PV. 25050–9 in cranial (I1), lateral (I2) and anterior (I3) views. *Antifer ultra,* antler remains (J–M). Proximal fragment of an antler SGO.PV.25,054, in medial (J1) and lateral (J2) views. Basal fragment of an antler's second tine SGO.PV.25,052 in medial (K1) and lateral (K2) views. Pedicle of an antler SGO.PV.25,051 in medial (L1) and lateral (L2) views. Nearly complete right antler SGO.PV.26,045 in medial (M1) and lateral (M2) views. Scale bar for A = 5 cm. Scale bar for B-D, G-I = 10 cm. Scale bar for E-F = 5 cm. Scale bar for J-L = 20 cm. Scale bar for M = 40 cm.

remains are assigned only at the family level since all the diagnostic features defined for the two recognized genera of gomphotheres in South America, *Cuvieronius* and *Notiomastodon* (Mothé et al., 2017), are located mainly in the skull and tusks (Alberdi et al., 2002; Mothé et al., 2017). MNI = 2 is estimated.

4.1.6.2.2. Order Carnivora Bowdich, 1821

4.1.6.2.2.1. Family Canidae Fischer De Waldheim, 1817

4.1.6.2.2.1.1. Genus Lycalopex Burmeister, 1854

4.1.6.2.2.1.1.1. Lycalopex culpaeus Molina, 1782 (Figs. 7A and 9A, Table 1, Appendix B and C)

Only a posterior segment of a right mandible of an adult canid was recovered. It has no teeth and only the alveoli of m1-m3 and the posterior alveolus of p4 are preserved. The metric analysis suggests that the mandible exhibits a size smaller than *Dusycion avus* Burmeister from Patagonia, being compatible with the genus *Lycalopex* (Fig. 9A, Appendix C). It has been suggested that *L. culpaeus* has an average size and weight greater than *Lycalopex griseus* (Iriarte, 2008). The metric data used as comparison agrees with the above and allows the inclusion of the fossil specimen in *L. culpaeus.* MNI = 1 is estimated.

4.1.6.2.3. Order Perissodactyla Owen, 1848

4.1.6.2.3.1. Family Equidae Gray, 1821

4.1.6.2.3.1.1. Genus Hippidion Owen, 1869

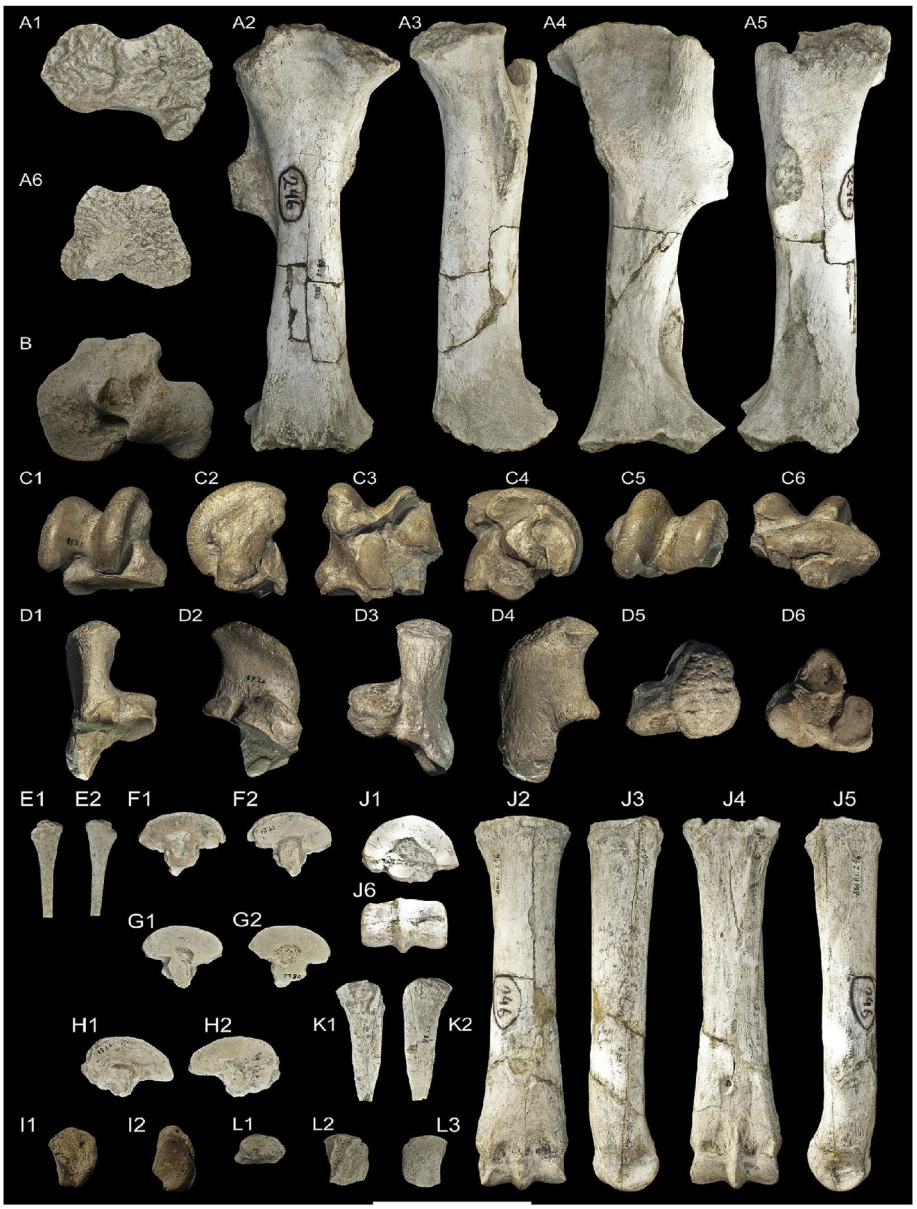

Fig. 8. Remains of *Hippidion principale* from Taguatagua 1 site. Right unfused femur SGO.PV.246-a. In proximal (A1), cranial (A2), medial (A3), caudal (A4), lateral (A5) and distal (A6) views. Proximal unfused tibia SGO.PV.25,555 in proximal (B) view. Right astragalus TT-58 in dorsal (C1), medial (C2), plantar (C3), lateral (C4), proximal (C5) and distal (C6) views. Right calcaneus TT-67 in dorsal (D1), medial (D2), plantar (D3), lateral (D4), proximal (D5) and distal (D6). Proximal right metacarpal II SGO.PV.25,554 in medial (E1) and lateral (E2) views. Right tarsal III SGO.PV.26,043 in distal (F1) and proximal (F2) views. Right tarsal III SGO.PV.26,044 in proximal (G1) and distal (G2) views. Central tarsal SGO.PV.26,042 in proximal (H1) and distal (H2) views. Proximal sesamoid SGO.PV.25,556 in lateral (I1) and dorsal (I2) views. Right metatarsal III SGO.PV.246-b in proximal (J1), dorsal (J2), medial (J3), plantar (J4), lateral (J5) and distal (J6). Diaphysis and proximal right metatarsal IV SGO.PV.25,558 in medial (K1) and lateral (K2) views. Proximal right metatarsal IV SGO.PV.25,557 in medial (L1) and lateral (L2) views. Scale bar = 10 cm.

4.1.6.2.3.1.1.1. Hippidion principale Lund, 1846 (Figs. 8 and 9C, Table 1, Appendix B and D)

Eleven bones are referred: an unfused right femur, a proximal tibial epiphysis, a right astragalus, a right unfused calcaneus, a right proximal metacarpal II, a right central tarsal, two tarsal III, right complete metatarsal III, two proximal right metatarsals IV, and a proximal metacarpal II. The presence of an unfused femur and a tibia suggests an age-at-death of 3–3,5 years, according to epiphyseal fusion in *Equus ferus caballus* (Silver, 1963). Tarsals and metatarsal III articulate each other. The specimens belong to equids considering the presence of a well-developed metatarsal III and the presence of a small rudimentary metacarpal IV. Particularly, in the proximal tibial epiphysis, the lateral intercondylar tubercle is slightly cranially projected and is located comparatively more posterior than the medial tubercle (that is, they are not aligned) (Fig. 8B). In a *E. ferus caballus* comparative specimen, both tubercles are aligned. The medial tubercle is a well-defined cranial projection, rounded and clearly separated from the lateral tubercle by a pronounced oval fossa, oriented obliquely. This fossa is noticeably smaller in *Equus*. Another interesting feature was observed in both tarsal III since distally they show only one single irregular facet for the metatarsal III (Fig. 8F and G). The morphology of the facet is unusual given that in *E. caballus* the distal surface is divided into two facets.

The size and robustness of the specimens analyzed suggest the presence of a *Hippidion* species. Some unusual features not seeing

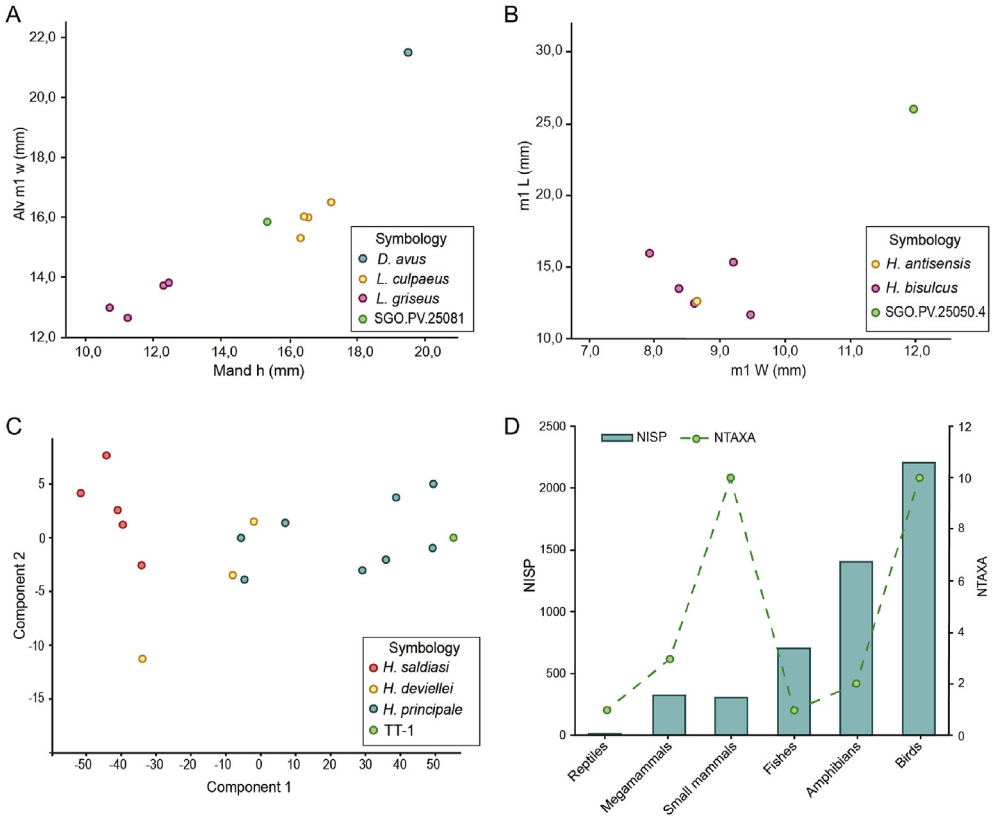

Fig. 9. Measurements of different Canidae mandibles and SGO.PV.25,081; Alv m1 w: width of the alveolus of the m1; Mand h: height of the mandible behind m1 (A). Measurements of different Cervidae mandibles and SGO.PV.25,050–4; m1L: length of m1; m1W: width of m1 (B). Principal component analysis considering metatarsal III measurements. Component 1 explains 96,78% of the variance. See Appendix D for data employed (C). Diagram of NISP and NTAXA (D). Data taken from Table 1.

in *Equus* (i.e. the situation of the intercondylar tubercles, the morphology of the distal facet of tarsal III) deserve further study in order to evaluate its taxonomic significance. The PCA conducted with measurements from the metatarsal III (Appendix D), clearly allows its inclusion in *H. principale* (Fig. 9C). These results agree with previous osteometric analysis performed by Alberdi and Frassinetti (2000). Considering the epiphyseal fusion and its laterality, most of the material described belongs to the rear limb of a young single individual. A second individual is represented in the assemblage by fewer elements.

4.1.6.2.4. Order Artiodactyla Owen, 1848

4.1.6.2.4.1. Family Cervidae Gray, 1821

4.1.6.2.4.1.1. Genus Antifer Ameghino, 1889

4.1.6.2.4.1.1.1. Antifer ultra Ameghino, 1889 (Fig. 7J-M, Table 1, Appendix B, E)

Three antler fragments and a nearly complete antler were recovered. The most complete specimen has a subcircular base with the burr surrounded by small tubercles (Fig. 7M). The pedicle is straight until it reaches the first tine, which is almost perpendicular to the beam axis. The first ramification is bifid and compressed. The lower tip is smaller than the upper, probably due to its usage. After the first tine, the beam becomes transversally compressed. The second tine is obliquely oriented to the beam. The beam continues with a sub-quadrangular section until it reaches the third and fourth tine. The antler is covered by numerous parallel striae and grooves. All the fossil antlers share the same general morphology. These characters have been proposed for *A. ultra* (Alcaraz, 2010; Labarca and Alcaraz, 2011). The measurements obtained point out in the same direction since are consistent with each other and compatible with metrical data from Labarca and Alcaraz (2011) (Appendix E). MNI = 1 is estimated.4.1.6.2.4.1.2. Cervidae indet. (Fig. 7B–I, 9B, Table 1, Appendix B and F)

Nine specimens were identified including a left maxillary portion, three mandibular fragments, left and right m1, a left radius diaphysis, a proximal left ulna and a distal diaphysis of a radius. The maxilla retains the Dp3 and Dp4 (Fig. 7B). The occlusal surface show typical selenodont features. In the Dp3 the anterior loph is extended anteroposteriorly. The metastyle is in contact with the labial segment of the posterior loph. Dp4 exhibits a mesoestyle labially projected, more developed than the parastyle. The protocone is angled. In the complete m1 (Fig. 7E), the anterior lophid is extended anteroposteriorly. The posterior lophid is more angled than the anterior. The metastylid and the parastylid are projected lingually, although the latter is less pronounced. In the mandible, the ramus body retains the pd3 and pd4 (Fig. 7C). The pd2 is absent. The alveolus of m1 is nearly complete and left m1 fits in. The pd3 has three lophid, increasing this size of its from anterior to posterior. It has two ectostylid (anterior and posterior) which are divergent in orientation. Metastylid and entostylid are well projected. The pd4 possess an anterior valley well excavated. The medial valley is smaller than the anterior, triangular, surrounded by a metaconid and posterocristid well developed. The hypoconid is also triangular and is connected to the protoconid by a small bridge (external postprotocristid) due to its wearing. All the molar and mandibular fragments probably belong to a single element. According to tooth eruption sequence and wear for *Dama dama* (Brown and Chapman, 1990), and *Cervus elaphus* (Azorit et al., 2002), the mandible could belong to a very young juvenile individual, ~4 months old at-the-time-of-death. The postcranial remains (radius and ulna) are unfused proximally (Fig. 7H and I). In

Table 1
Summary of taxa identified from Taguatagua 1 site. *: New taxon for the chilean Pleistocene.

Class	Order	Family	Taxon	NISP	MNI
Gastropoda	Pulmonata	Planorbidae	*Biomphalaria taguataguensis*	3	3
Actinopterygii	Atheriniformes	Atherinopsidae	*Odonthestes* sp.*	5	2
			Atherinopsidae indet.	16	3
			Actinopterygii indet.	681	
Lyssamphibia[+]	Anura	Calyptocephalellidae	*Calyptocephalella gayi*	840	92
		Bufonidae	*Rhinella* sp.	1	1
			Anura indet.	559	
Reptilia	Squamata	Dipsadidae	cf. *Philodryas* sp.*	4	1
Aves	Anseriformes	Anatidae	cf. *L. specularioides**	2	1
			Anas cf. *A. flavirostris**	3	3
			Anas cf. *A. georgica*	3	2
			Anatidae indet.	105	
	Podicipediformes	Podicipedidae	*Podiceps major**	2	1
			Podicipedidae indet.	2	2
	Columbiformes	Columbidae	*Zenaida* sp.*	1	1
			Columbidae indet. *	1	1
	Gruiformes	Rallidae	*Fulica* cf. *F. rufifrons**	1	1
			Fulica cf. *F. armillata**	1	1
			Rallidae indet.	2	
	Accipitiformes	Accipitridae	*Geranoaetus melanoleucus**	1	1
	Falconiformes		*Milvago* cf. *M. chimango**	1	1
			Aves indet.	2085	
Mammalia	Didelphimorphia	Didelphidae	*Thylamys* sp.*	1	1
	Proboscidea	Gomphotheriidae	Gomphotheriidae indet.	19	2
	Carnivora	Canidae	*Lycalopex culpaeus*	1	1
	Perissodactyla	Equidae	*Hippidion principale*	11	2
	Artiodactyla	Cervidae	*Antifer ultra*	4	1
			Cervidae indet.	9	1
			"Megafauna" indet.	283	
	Rodentia	Octodontidae	*Octodon bridgesii**	4	3
			*Octodon degus**	51	11
			Octodon cf. *O. lunatus**	6	4
			*Aconaemys fuscus**	4	2
			Spalacopus cyanus	4	3
			Octodon sp.	16	6
			Octodontidae indet.	12	
		Abrocomidae	*Abrocoma bennettii*	2	2
			Abrocoma sp.	2	1
		Echimyidae	*Myocastor coypus*	11	2
		Cricetidae	*Abrothrix* cf. *A. longipilis*	2	1
			Cricetidae indet	8	
			Rodentia indet.	222	
Undetermined	bones			1656	
Total				6647	160

[+]: Not formally ranked. Underlined the extinct or locally extirpated taxa.

C. elaphus the proximal radius fuses at 8-month-old, so the fossil specimen belongs to a younger individual.

The measurements obtained for the m1 are larger than those obtained for *Hippocamelus bisulcus* and *Hippocamelus antisensis*, the biggest cervids living at present in Chile (Fig. 9B, Appendix F). The statement above suggests the presence of an extinct form, probably *Antifer* considering its record in the same stratigraphic context. Unfortunately, all the known diagnostic features of this genus are located in the antlers (Alcaraz, 2010). All the fossils probably belong to a single very young individual (MNI = 1).

4.1.6.2.5. Order Rodentia Bowdich, 1821

4.1.6.2.5.1. Family Octodontidae Waterhouse, 1839

4.1.6.2.5.1.1. Genus Octodon Bennet, 1832

4.1.6.2.5.1.1.1. Octodon degus Molina, 1782 (Fig. 5E and F, Table 1, Appendix B)

Fossils of *O. degus* are common in the sample and include 51 specimens (Table 1). The specimen identified correspond to several upper (NISP = 13) and lower (NISP = 15) isolated molars, maxillary fragments (NISP = 8), and mandibles (NISP = 15). In general, P4-M2 have very shallow mesoflexi, which only occurs in *O. degus*. This pattern is observed also in very young individuals of *Octodon* spp., but all the fossils belong to adult individuals (with M3 erupted). Regarding lower dentition, the fossils are included in *O. degus* considering the following traits: a short protoconid, along with a short mesoflexid and a well-defined globular-like paraconoid. MNI = 11 is calculated.4.1.6.2.5.1.1.2. *Octodon bridgesii* Waterhouse, 1845 (Fig. 5G and H, Table 1, Appendix B)

The material assigned to Bridges's degu consists of two molars and two mandibles with teeth (p4-m2). The p4, m1, and m2 have a deep and very broad mesoflexid, feature only observed in *O. bridgesii* and *O. lunatus*; being deeper and broader in the former. The metaconid, in its posterior wall, presents a more angular form, shaping the posterior lobe with a square-like figure. Such a pattern is only seen in *O. bridgesii* since *O. lunatus* presents a comparatively more rounded form (Hutterer, 1994). In this fossil, the orientation of the labial enamel wall extends from the paraconid until it reaches the protoconid. In *O. lunatus* forms a straight line, while in *O. bridgesii* shows a "breakpoint" in its angle (Hutterer, 1994; Osgood, 1943; Reise, 1973). All the molariforms present a deep hyploflexi, with abundant cement, features not seen in *O. lunatus*. MNI = 3 is estimated.4.1.6.2.5.1.1.3. *Octodon* cf. *O. lunatus* Osgood (1943) (Fig. 5I, Table 1, Appendix B)

Six specimens are identified: a left mandible with teeth included (p4-m1), two isolated lower molars, a right m1, and a right m2.

Lower molars, m1 and m2, are conferred to *O. lunatus* considering the prolongation, orientation, and shape of their crowns and the flexids. The protoconid is larger in *O. lunatus* and exhibits a deeper mesoflexid. Also, the medial enamel wall that connects the protoconid with the paraconid lacks a "break-point" in its contour, feature only observed in *O. degus* (Hutterer, 1994). Nevertheless, careful study of the reference specimens suggests high variability in the diagnostic traits of *O. lunatus*, some of them becoming very close to the observed in *O. degus*. This situation permits only the use of an open diagnosis. MNI = 4 is estimated.4.1.6.2.5.1.2. Genus *Aconaemys* Ameghino, 18914.1.6.2.5.1.2.1. *Aconaemys fuscus* Waterhouse, 1842 (Fig. 5K, Table 1, Appendix B)

Four specimens belong to the Chilean rock rat: a left P4, a right p4, an unidentified molariform, and a left mandible fragment with p4. The upper premolar has the typical eight-shape form of the Octodontoidea superfamily, with two main lobes connected through a medial bridge (Patton et al., 2015). Both p4 show features characteristic of *Aconaemys* genus: the extremely narrow bridge that separates the hypoflexid and mesoflexid, in which both enamel walls are in contact with each other, and a hypoflexid deeper than the mesoflexid (Patton et al., 2015). The specimen corresponds to a p4 because the distal oval lobe is smaller than the mesial triangular one. The unidentified molariform is broken conserving only an oval lobe, in which the hypoflexid enamel reaches the wall of the mesoflexi enamel, without dentine between them. This feature is diagnostic for the *Aconaemys* genus. While *A. porteri* is distinguished from its very narrow lobes, with extended paraconids and metaconids, *A. sagei* is very similar to *A. fuscus* in its occlusal pattern, but the former is smaller (Gallardo and Reise, 1992). Also, *A. sagei* has a paracone/paraconid and metacone/metaconid more extended that *A. fuscus*, but not as exaggerated as in *A. porteri*. MNI = 1 is estimated.4.1.6.2.5.1.3. Genus *Spalacopus* Wagler, 18334.1.6.2.5.1.3.1. *Spalacopus cyanus* Molina, 1782 (Fig. 5J, Table 1, Appendix B)

A right mandible fragment, two right M1 and one M2 are included in *S. cyanus*. The mandible includes the ramus, the incisor alveolus, the anterior part of the angular process and the molariforms p4, m1 and m2. In the lower molariforms, the bridge between the mesoflexid and the hypoflexid are open, with a broad space of dentine, a feature observed in *Spalacopus*. The distal lobe of the inferior molariforms has an oval-shape similar to those observed in the superior dental series. All the molariforms exhibit a triangular shape in its mesial lobe, but less angular as in *Aconaemys*. MNI = 3 is estimated.

4.1.6.2.5.2. Family Abrocomidae Milled and Gidley, 1918

4.1.6.2.5.2.1. Genus Abrocoma Waterhouse, 1837

4.1.6.2.5.2.1.1. Abrocoma bennettii Waterhouse, 1837 (Fig. 5L, Table 1, Appendix B)

This taxon is represented by two left mandibles. The first one includes the ramus, which is much larger compared with Octodontidae rodents. The premolar specimen is complete. In occlusal view, it has deep mesoflexids and hipoflexids. The shape and form of their protoconid, hypoconid, metaconid, entoconid, and posterolophid are similar to those observed in the specimens of *A. bennettii* used as reference. It differs from *A. cinerea* since this taxon presents thick dentine in the bridges between the cusps, where the labial enamel does not contact the lingual enamel (Verzi and Quintana, 2005), and also in a more obtuse angle of the entoconid and metaconid. In contrast, *A. cinerea* has more angled vertices in their lobes. The second left mandible extends from the incisor alveolus to the anterior segment of the ramus. It only preserves the alveolus of the premolar, with a clear shape of an *Abrocoma* tooth, along with a prolonged and thin incisor alveolus. MNI = 2 individuals are calculated.

4.1.6.2.5.3. Family Echimyidae Gray, 18254.1.6.2.5.3.1. Genus Myocastor Kerr, 17924.1.6.2.5.3.1.1. Myocastor coypus Molina, 1782 (Fig. 5B–D, Table 1, Appendix B)

Eleven bones of *M. coypus* are identified: an upper right incisor fragment, a left M3, a right p4, a right m3, an unidentified molariform, a left scapula; two right tibiae, a left calcaneus, and a first phalanx. The size of the incisor is similar to *M. coypus* used as reference. The p4 was included in *M. coypus* considering the number of flexi in each toothrow: the lower molariforms have one flexid in its buccal side and three in its lingual side, meanwhile, the upper molar has two flexi in its palatinal side and three in its buccal side. Two m3/M3, lower right, and upper left respectively present crowns flattered, with simplified flexi, compatible with *M. coypus*, being traits of a worn tooth. The unidentified molariform only retains a complete oval cuspid with a very deep flexi and a small portion of another cuspid.

Regarding postcranial fossils, the ventral fragment of a scapula retains the glenoid fossa, the neck, and the supraglenoid tubercle. The fragment includes the more ventral portion of the scapular blade and the acromion. The tibiae size, and the position and shape of its condyles and tibial tuberosity are identical to those observed in the *M. coypus* reference material. In distal view, the medial and lateral malleolus have the same angle as in the reference material, with a groove for the tendon of tibialis posterior with the same depth and extension, especially the posterior talar articular surface. About the calcaneus and phalanx, both are similar in shape and size to *M. coypus* comparison material. MNI = 2 is calculated.

4.1.6.2.5.4. Family Cricetidae Fischer, 1817

4.1.6.2.5.4.1. Genus Abrothrix Waterhouse, 1837

4.1.6.2.5.4.1.1. Abrothrix cf. A. longipilis Waterhouse, 1837 (Table 1, Appendix B)

The long-haired grass mouse fossils identified are a left mandible with two molariforms (m1-m2) and a right mandible with all their molars. In both specimens, the m1 has a fan-shaped procingulum, a shallow or absent anteroflexid. The m2 has a "three shape", with deeps flexi, a 90°-degree procingle, and two oblique parallels metaconid and entoconid. The m3 has a 90°-degree procingle, like in m2, but with a down-pointed arrow-shape hypoconid, which has only been observed in this species. The coronal topography is crested, which is typical in juveniles, while in adults they tend to be flat and lose some morphological structures (Fernández et al., 2011; Patton et al., 2015; Teta, 2013). MNI = 1 is estimated.

4.2. Quantification and taphonomy

A total of 6,647 specimens were analyzed and 75% of the sample was identified at least to Class level. Most of the specimens belong to small taxa such as birds, amphibians, fishes, and rodents (Table 1). Twenty-eight non-inclusive taxa were identified, being the Class Aves the richest group (NTAXAbirds = 10), followed by Rodentia (NTAXArodents = 8). Inversely, anurans and freshwater fishes are the less rich groups (NTAXAanurans = 2, NTAXAfishes = 1) (Table 1). Higher richness is usually correlated with sample size (Lyman, 2008), which is not strictly the case here (Fig. 9D). Anurans registered the highest number of individuals (MNIanurans = 93), followed by rodents (MNIrodents = 31).

In mammals, weathering seems to act differently in the sample, since a canid mandible (Fig. 10A) and some of the gomphothere bones (i.e mandible, pelvis, Fig. 6B, F) shows initial longitudinal cracking associated to an early stage of weathering, but other bones (i.e. fíbula, tibia, astragalus, Figure H–J) show no weathering signals. Horses and cervids are not weathered. Weathering seems not to be important in the rodent assemblage. In contrast, polished/

Fig. 10. Surface bone modification on small fauna remains from Taguatagua 1 site. Dentary fragment of *Lycalopex culpaeus* SGO.PV.25,081 with roots marks superimposed over weathering (A). Distal humerus fragment of an Anatidae indet. SGO.PV.26,441 with its diaphysis partially blackened due manganese (B). Distal humerus fragment of Anatidae indet. SGO.PV.23,362 with roots marks superimposed over manganese stain (C). Dentary fragment of *Abrocoma bennettii* SGO.PV.25,637 with moderate polishing (D). Distal humerus fragment of a medium-sized caviomorph rodent SGO.PV.25,660 with an intensive thermal alteration (E). Clavicle of *Calyptocephalella gayi* SGO.PV.26,253 with slight polishing and isolated circular manganese stains (F). Distal coracoid fragment of Anatidae indet. SGO.PV.26,180 with root marks superimposed over thermal alteration (G). Distal femur fragment of Anatidae indet. SGO.PV.26,265 with gastric corrosion (H). Anterior sternum fragment of an indet. bird SGO.PV.26,264 with cracking with curled up edges located near to *spina interna rostri* (I). Scale bar for A, B and D = 20 mm. Scale bar for C, E, F–I = 10 mm.

abraded bones are common in small fauna (Fig. 10D, F), ranging from bones with a slightly smooth surface to specimens with rounded edges and exposure of cancellous bone (Fernández-Jalvo and Andrews, 2003). Some bird and rodent bones show digestive corrosion (Fig. 9H), reflected mainly in pitting and cracking (Andrews, 1990). Manganese coating is common in the small fauna assemblage, especially in fishes, birds, and anurans (Fig. 10B, F). In contrast, in megafauna, this alteration is practically absent. The presence of different types of pigmentation, ranging from small isolated circular stains (type 1) to heavily blackened (type 4) was observed (Marín-Arroyo et al., 2008). Other conspicuous modifications detected mainly in small taxa were cracking with curled up edges (Fig. 10I) (Fernández-Jalvo and Andrews, 2016) and circled whitish areas on the bone surface due to bioerosion (Pesquero et al., 2010).

Root marks were registered in different taxonomic groups (cervid, canid, horses, rodents, birds) but usually in isolated patches and not covering extensive bone areas. These marks are mainly superficial. In some cases, root marks are superimposed to manganese coating, thermoalteration and weathering (Fig. 10A, C, G). So far, no rodent or carnivore marks have been observed.

Clear anthropic marks were only detected in megamammal bones. A long bone diaphysis of Cervidae indet. exhibits a green fracture and a negative impact in one of its edges. There is a flake scar in the medullary cavity (Fig. 11A). A mandible probably belonging to the same individual exhibits seven parallel cut marks in its condylar process, oriented anteroposteriorly, suggesting dismemberment activity (Binford, 1981) (Fig. 11C). A horse astragalus and a calcaneus show cut marks in their lateral face (Fig. 11B, D). Both marks represent one single butchering activity (Casamiquela, 1976; Montané, 1968). One unidentified rib fragment shows two sub-parallel cut marks. No cultural marks were observed in gomphothere or smaller taxa. Finally, we have detected some rodents, birds and anurans burned bones (Fig. 10E) however, the frequency of these elements is low. No thermal alteration has been recorded in large mammals.

5. Discussion

5.1. Taxonomy

So far, no other late Pleistocene archaeological or paleontological deposit in Chile has a taxonomic richness such as TT-1, with 28 different taxa, including placentals, marsupials, anurans, reptiles, birds, fish, and gastropods. This is because late Pleistocene faunal studies have been historically focused on megafauna, probably due to its easy-to-recover bias against microfaunal remains (Labarca, 2015).

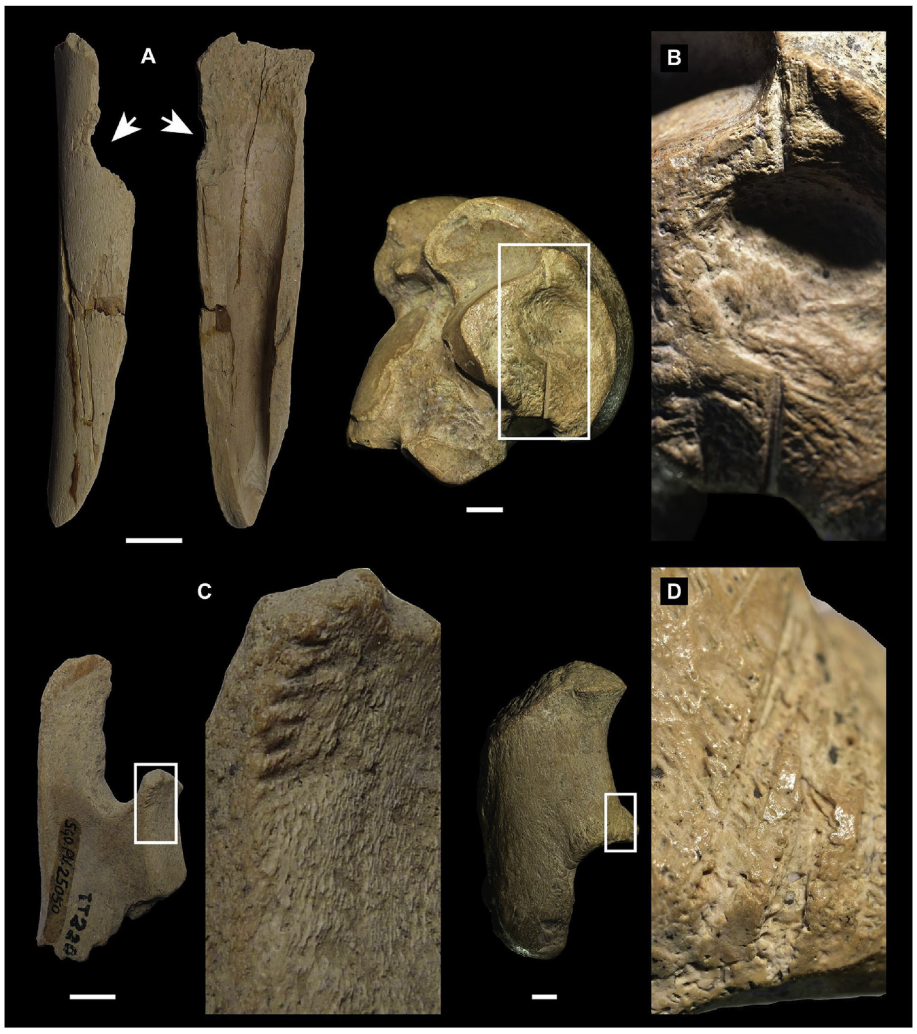

Fig. 11. Human-induced modifications on megafauna remains from Taguatagua 1 site. Long bone diaphysis of Cervidae indet. SGO.PV.25,050–10 with a negative impact and negative scar (A). Astragalus of *Hippidion principale* TT-58 with cutmarks on its lateral face (B). Ramus fragment of Cervidae indet. SGO.PV.25,050–7 with cutmarks on its condylar process (C). Calcaneus of Hippidion principale TT-67 with cutmarks in its sutentaculum tali (D). Scale bars = 10 mm.

Our taxonomic analyses showed that most of the taxa identified (85,7%) were ~10 kg mass or less, suggesting a faunal Pleistocene richness for Central Chile based on small animals rather than megamammals. This situation would have been stressed after the late Pleistocene-Holocene extinction of megafauna and persists until today. Most of the taxa identified are associated with lacustrine and/or freshwater deposits such as Anatidae, Podicipedidae, Rallidae, Calyptocephalellidae and Echimyidae. The lacustrine context would also explain the high NISP of anurans and anatins.

Sixteen identified taxa (57,1%) are new for the late Pleistocene fossil record of Chile (Table 1), including two previously unregistered orders, which also have a sparse record in South America, such as Squamata and Atheriniformes (Albino, 1999; Bogan et al., 2009; Camolez and Zaher, 2010; Hoffstetter, 1968; Porta, 1965; Scanferla et al., 2005). The chilean late Pleistocene bird fossil richness improves up to 29% after this study, with nine unregistered taxa, including two ducks, two coots, one grebe, two pigeons, one eagle and one caracara (Table 1, Appendix G). These records make of Laguna de Tagua Tagua the richest Chilean late Pleistocene locality in terms of ornithological fauna. The four recorded octodontids in TT-1 expand in 33% the Chilean caviomorph late Pleistocene record (Appendix H). Moreover, the stratigraphic association of five of the nine known extant octodontids in Chile has not been recorded previously during the Pleistocene. TT-1 also corresponds to the only late Pleistocene Chilean and South American deposit with a high concentration of *Calyptocephalella gayi* individuals, including different ontogenetic stages. Considering the fragmented condition of the remains and the absence of critical reference collections, it is very possible that this faunal list will improve in the future, particularly the class Aves, in which several unidentified morphotypes were detected (Alarcón, 2016). The patterns of richness identified in the fossil assemblage are in agreement with the current taxonomic richness of Chile, in which birds are the most abundant vertebrate group (Jaramillo, 2005; Victoriano et al., 2006).

So far, no extinct small fauna were identified in the assemblage, but there is evidence of three locally extirpated taxa. The Crested duck *Lophonetta specularioides* is currently distributed in the andean range from 35° to 46°S (Bulgarella et al., 2007; Navas and Bo, 1998), however, in the southernmost portion of its distribution, is also present in coastal areas (Jaramillo, 2005). Also, *Octodon* cf. *O. lunatus* and *Aconaemys fuscus* were apparently locally extirpated from the area during the Holocene, probably due to anthropic factors (Saavedra and Simonetti, 2003).

Only the megafauna (gomphotheres, equids and cervids) identified in TT-1 became extinct at the Pleistocene-Holocene transition (Barnosky and Lindsey, 2010; Cione et al., 2009). Considering the radiocarbon dates reported for this site (and particularly for TT-2) as bracketing dates for the stratigraphic presence of megafauna, it is possible to notice that these are placed among the youngest in Chile and South America. For example, the youngest taxon ^{14}C date on record in the continent for a Gomphothere is one of 11,890 cal yr BP coming from southern Chile (Chan Chan, 40°S-73°W, Gonzalez-Guarda et al., 2018), followed by dates of 12,230 cal yr BP (Poço Redondo, Sergipe, Brazil, 9°S-37°W, Silva, 2008) and 12,650 cal yr BP (Arroyo Chasicó, Provincia de Buenos Aires, Argentina, 40°S-66°W, Prado et al., 2015). Taxon dates known for *Hippidion principale* are all between 15,300–18,340 cal yr BP (five dates, Buenos Aires province, Argentina, Prado et al., 2015) being much older than the age range of TT-1 and TT-2. This opens the possibility of interpreting central Chile and LTT as refugia for the vanishing megamammals adapted to cold and wet environments (Núñez et al., 1994). More taxon dates on the faunas recovered from LTT is needed to test this hypothesis.

5.2. Taphonomy and deposition environment

Megafauna and small faunal fossils were recovered in spatial association with lithic and bone artefacts. Nevertheless, according to radiocarbon dates, the human occupation seems to be archaeologically discrete, making possible to suggest a mixed fossil assemblage in which natural and cultural events were combined in the sedimentary matrix. Taphonomic analysis could help to evaluate the origin of the different taxa identified (Gifford-González, 1991).

Regarding the megafauna, the low-energy sedimentary context reported (fine siliciclastic silt, Valero-Garcés et al., 2005) is not compatible with fluvial or colluvial deposition of the fossils. Given the weight of the bones of these taxa, especially those of gomphotheres (Haynes, 1991), a great hydraulic force is required to displace them (Frison and Todd, 1986). Also, the bones are not abraded or polished. Natural death in this kind of context would leave relatively complete and articulated carcasses (Hill, 1979). Both Casamiquela (1976) and Montané (1968) indicated that no articulated big mammal bones were identified. Secondary processes, such trampling, could subsequently disarticulate this kind of context, but no trampling marks have been detected in the sample analyzed. A carnivore kill-site is also rejected since no tooth marks were identified on the bones. Actualistic studies suggest that big felids leave tooth marks in the bones during consumption of middle-size carcasses, mainly in the ribs and long bone epiphysis (Domínguez-Rodrigo, 1999; Gidna et al., 2014, among others), even if they have primary access to the prey. Tooth marks in the bones increase in quantity and distribution along the bones in a scavenging scenario (Gidna et al., 2014). Also, paleontological evidence has shown that north and south American Pleistocene Machairodontinae and Felidae taxa left tooth marks during bone consumption (e.g. Martin, 2013; Marean and Ehrhardt, 1995).

Since the fossils are differently weathered is possible to assume differential bone deposition and/or different burial events. In any case, some of the big mammal bones were exposed on the surface prior to its final burial. In spite of this, the bones are not tooth marked.

The anthropic marks observed in horse and cervid bones suggest that these taxa were culturally deposited. The absence of cut marks in gomphothere bones does not invalidate a possible cultural deposition since ethnographic and actualistic research with extant proboscideans (Haynes, 1987, 1991; Haynes and Klimowicz, 2015) indicate a very low proportion of cut-marked bones during butchering processes. Nevertheless, Casamiquela (1976) informed the presence of splintered tusk fragments scattered around the site, interpreting them as an intentional removal of the incisors, which are not found in the assemblage. Some of the horse (tarsals and metatarsal) and gomphothere (tibia, fibula, and calcaneus) bones articulate with each other, indicating that specific complete skeletal segments, rather than complete carcasses, were transported articulated to the camp to be further processed, including disarticulation, marrow extraction and probably tool production. Coincidentally, the lithic studies suggest mainly cutting and scraping activities on soft objects (Méndez, 2015).

Finally, the almost total absence of manganese coated bones and other water induced modifications among the megamammal remains indicates that the fossils probably were not buried in a saturated environment after its deposition (Marín-Arroyo et al., 2014), and it would also indicate mainly dry episodes after the camp was abandoned. Root marks in a weathered canid mandible supports this scenario.

The small fauna assemblage includes freshwater taxa (such as anatids and fish), mainly shore taxa (such as coypo) but also dry-land taxa (such as snakes and fossorial rodents), which suggests a strongly time-averaged assemblage and accounts for the fluctuations in the lake level prior, during and after the human occupation. Casamiquela (1976) pointed out that no articulated skeletons of small fauna were recovered during the excavations, and therefore the in situ natural death of, for example, fossorial rodents can be discarded. The presence of rodent and bird bones with digestive traces suggest that an undetermined portion of both groups could have entered the deposit by means of raptor pellets or scats posteriorly disaggregated. Most of the rodent taxa identified, such as *S. cyanus*, *A. bennettii*, *O. bridgesi*, and *A. fuscus* are nocturnal or crepuscular (Iriarte, 2008), but so far, only diurnal raptors have been determined (*Milvago* cf. *M. chimango* and *Geranoaetus melanoleucus*). *Lycalopex culpaeus*, on the other hand, usually preys upon these taxa (Correa and Roa, 2005; Jaksic et al., 1980; Torres, 2007) and could have contributed to the inclusion of rodents in the assemblage.

Natural deposition of fish bones is common in lacustrine contexts (Stewart, 1991), and the same would be expected for water birds such as ducks and coots. The presence of these taxa suggests high lake levels, and therefore more humid conditions. The presence of manganese coating almost exclusively in small fauna bones, including dry-land taxa (rodents) and freshwater taxa (anurans, birds and fishes), are indicative of an organic-rich sedimentary matrix capable of staining the bones (Marín-Arroyo et al., 2014), like a lake-shore environment, and suggest that its deposition could be not synchronic with the human occupation. Bones exhibiting cracking with curled up edges and circled whitish areas similar to those observed in TT-1 sample have been described in submerged environments elsewhere (Fernández-Jalvo and Andrews, 2016; Pesquero et al., 2010). The polished/abraded bones detected in the sample analyzed are coherent with this scenario, since small fauna exhibits this feature in water saturated clay/silty matrix (Fernández-Jalvo and Andrews, 2003; Griffith et al., 2016).

Some bones showed a combination of modifications, reflecting lake-level dynamics during the fossil deposition and burial. For example, some small fauna specimens show a combination of digestive corrosion and manganese staining, interpreted as an increment of the lake level after the bones were defecated and/or regurgitated. In contrast, the presence of roots marks superimposed to manganese stains and thermoalteration is interpreted as dry conditions once the bones were already buried.

No cultural marks were observed in the small fauna remains.

Nevertheless, cut marks and other human-induced modification are usually sparse in these bone assemblages (Hesse, 1984; Lloveras et al., 2009; Stahl, 1996). Taphonomic processes also can obscure anthropic modifications (Nicholson, 1996). Some of the taxa identified have a considerable mass and, in later times, were exploited by prehistoric groups that inhabited LTT, such as *Myocastor coypus* and *Calyptocephallela gayi* (Jackson et al., 2012). Anatidae exploitation has also been reported in late Pleistocene archaeological sites in southern Patagonia (Labarca, 2016). A few burnt bones would suggest human consumption of these taxa, but a campfire located over previously natural deposited bones could create the same pattern.

In sum, all the evidence suggests a mainly natural-induced deposition of small fauna, prior, during and after the human occupation in a very dynamic shore-lake environment. In this line, taphonomic analyses also revealed different phases of lake-level increase/retraction of unknown duration and cyclicity.

5.3. Paleoecological, paleoenvironmental and paleoclimatic implications

From a regional and global perspective, TT-1 is contemporaneous with the beginning of the Younger Dryas event at ~12,700 cal yr BP, which is marked by a general transition from colder and wetter conditions to warmer and dryer environments (Moreno et al., 2018). This change is also associated with the end of the Antarctic Cold Reversal event (~14,700–12,700 cal yr BP, Moreno et al., 2018) and is anti-phased with the shift in the Northern Hemisphere from the warm Bølling-Allerød to the colder Younger Dryas. Drying and warming regional conditions coincide with the observations made for LTT, placing the events recorded at TT-1 within a transitional environment towards more restrictive water and food availability conditions for animals. Considering that this faunal assemblage represents a time-averaged assemblage during this critical and particularly fluctuating period, the expectation is to find a mixed faunal record comprising taxa of different habitat preferences.

Among the ducks, *Lophonetta specularioides* has a present-day distribution associated to cold conditions (Jaramillo, 2005) and its presence in TT-1 agrees with the latest humid/cold pulse during the LGT. Along with this cold-adapted bird, there are other taxa that currently inhabit semi-arid/Mediterranean environments. One of these is the marsupial *Thylamys*. Today *Thylamys pallidor* and *Thylamys elegans* are the only ones from the genus present in Chile; both live in semi-arid environments, although *T. elegans* is also distributed in Mediterranean areas (~37°S, Palma, 1997). Even, some physiological studies have shown that *T. elegans* could have adaptations to live in more temperate environments (e.g. Bozinovic et al., 2005). Thus, there is a possibility that this taxon could have inhabited TT-1 during a transitional environment. The same is true for *Octodon degus* which is the most abundant rodent identified in the assemblage. At present, *O. degus* inhabits arid, semiarid and Mediterranean environments (28°S-35°S, Patton et al., 2015), but a large number of studies have shown a broad range of behavioral plasticity in response to temperature and food fluctuations (e.g. Bacigalupe et al., 2003; Ebensperger and Hurtado, 2005; Kenagy et al., 2002; Lagos et al., 1995), and therefore its presence would be expected in more temperate/closed locations.

Other small taxa are not indicative of specific environments since its current distribution includes a variety of habitats. This is the case of the semifossorial rodent *Aconaemys fuscus*, which currently inhabits sandy areas covered with xerophytic vegetation as well as forested areas with *Nothofagus* (Iriarte, 2008). The above-mentioned plasticity is also applicable to the colubrid taxa identified since the genus *Philodryas* currently inhabits a wide variety of habitats ranging from the Atacama Desert to the Valdivian Forest (26°S-40°S, Donoso-Barros, 1966).

Probably the best bioindicator of the shift from colder and wetter to warmer and dryer environments is the mollusk *Biomphalaria taguataguensis*, since was only recorded in member 6 (Varela, 1976). *B. taguataguensis* inhabits minor small river environments with low to moderate runoff and a maximum depth of 1 m, associated with swampy local conditions (Covacevich, 1971).

Regarding the megafauna, the records of *Antifer ultra* in Argentina show a wide geographical and environmental distribution (25°S–38°S, Alcaraz, 2010; Alcaraz and Francia, 2013). This is also true for the late Pleistocene record in Chile, since the species has been found in warm and arid environments in central Chile (Quereo site; 31°S) (Labarca and Alcaraz, 2011), and in cold and humid environments in northwestern Chilean Patagonia around the same time period (Los Notros site; 40°S, Lira et al., 2020). Following this potential environmental plasticity and considering the absence of other proxies (e.g. isotopic data), the presence of *Antifer ultra* in TT-1 is not particularly informative.

Previous anatomical studies have concluded that *Hippidion* species have a greater adaptation to closed environments than *Equus* species (e.g. Alberdi et al., 2003). However, based on stable isotope studies in South America (Domingo et al., 2012; González-Guarda et al., 2017), both *Hippidion* and *Equus* were adapted to a diverse suite of environments, from closed-canopy forest to C_4-dominated grasslands. Specifically, *Hippidion principale* has been linked to woodland-mesic C_3 grasslands according to $\delta^{13}C$ values from dental enamel (Domingo et al., 2012). Thus, the vegetation transition in LTT during the formation of TT-1 could have been propitious for *H. principale* diet requirements.

Notiomastodon platensis is the only taxon from LTT that has been directly studied with the use of stable isotopes, dental microwear, and dental calculus (González-Guarda et al., 2018). A particular specimen (SGO.PV.47k) reported in González-Guarda et al. (2018) comes from an undetermined location in LTT and was radiocarbon dated between 13,810 and 14,520 cal yr BP, being slightly older than the deposits from TT-1 reported here. The sample shows coherence with previous paleoenvironmental and paleoclimatic interpretations obtained from continental (Heusser, 1983, 1990; Valero-Garcés et al., 2005) and marine sediments (i.e. alkenones; Kaiser et al., 2008), since this gomphothere was linked to a woodland-mesic C_3 grassland environment according to the $\delta^{13}C$ values obtained from the dental enamel bioapatite ($\delta^{13}C = -11.7‰$). According to the dental microwear and dental calculus analyses, the specimen exhibits a leaf browser diet (~100% consumption of trees) (González-Guarda et al., 2018). In addition, the mean annual temperature calculated from the oxygen isotope values from the same specimen was ~18 °C and similar to the sea surface temperature of the LGT (Kaiser et al., 2008). The mean annual precipitation calculated as well (702 mm) is similar to present-day values (Heusser, 1990). According to González-Guarda et al. (2018), the $\delta^{15}N$ values reported for the specimen from LTT are relatively high (8.4‰) when compared to others coming from other localities along central Chile. This value could suggest a drier environment, however, judging by the results of the multiproxy approach, we suggest that the nitrogen value could be due to other factors such as, fires, grazing intensity, and coprophagy and/or the fertilization of the vegetation located in regular migratory routes Metcalfe et al., 2013. Thus, the habitat of this particular *Notiomastodon platensis* in LTT was humid and wooded during the late Pleistocene which are consistent with its chronological position (see section 2.2.).

In sum, the presence in TT-1 of taxa with different environmental requirements seems to reflect the climatic/vegetational variations

reported for the Pleistocene-Holocene transition. High ecological plasticity suggested for several extant and possibly extinct taxa is coherent with this general trend. Nevertheless, the absence of detailed well-controlled faunal records prevents more robust conclusions and fine-grained comparison with other proxies.

6. Conclusions and future research

This analysis has revealed a particularly rich and complex lacustrine faunal community at the end of the Pleistocene in central Chile, which has no current analogous. It is composed mainly by taxa that currently inhabits the area, together with taxa that possibly extended/retracted its geographic range in response to climatic oscillations, but also with species that became extinct at the beginning of the Holocene. Our analysis showed the presence of several small taxa with scarce or null late Pleistocene fossil records in Chile and South America until now, which nevertheless are relatively common in current lacustrine environments. So far, no extinct small fauna have been identified in TT-1, suggesting that the Pleistocene-Holocene extinction affected exclusively large-bodied species.

This mixed faunal composition that includes taxa that currently inhabits semi-arid climates, together with taxa of temperate and/or cold requirements is explained by the time-averaged condition of the deposit, and therefore give us a coarse-grained picture of the faunal community variations during the Pleistocene-Holocene transition. The absence of detailed provenience information and recovery techniques of this assemblage prevents detailed discussions and comparison with other proxies but encourages us to continue working at this locality.

The taphonomic analysis is coherent with sedimentologic studies and points out a dynamic scenario during the Pleistocene-Holocene transition. Surface bone modifications suggest significant lake-level oscillations, which allowed the deposition of terrestrial, littoral, sublittoral and fluvial small fauna. In one of these lake-retraction moments the human presence in the LTT is recorded, reflected until now, exclusively by the exploitation of great size and greater caloric return taxa.

This research highlights the need of new detailed studies in LTT to characterize the faunal variations not only during the crucial Pleistocene-Holocene transition (member 5 to member 6) but in all the LTTF sequence. The future recovery of new well-documented faunal assemblages with robust chronologies will allow the development of more quantitative and therefore comparable analysis, opening the possibility to contrast new data with previously published paleoenvironmental proxies. Also, it will permit the use of non-morphological methodologies which would help us to reconstruct shorter environmental events over time (from months to tens of years); for example, the calculation of more precise temperature and precipitation values. Also, stable isotopes could define the seasonality of the diet in mammals (sequential sampling) and the migratory events in fossil birds. Finally, at a regional level, new systematic research must be conducted to detect and study novel fossiliferous deposits and therefore expand our knowledge of the late Pleistocene faunas in central Chile.

Author statement

RL and E.G.G designed the research, R.L., A.L.C, J.A.M., F.S.L., P.O.A., S.S.A. and K.E.B. undertook laboratory analyses, A.L.C, J.A.M., F.S.L. and S.S.A. carried out data curation, all authors contributed to writing the manuscript.

Declaration of competing interest

The authors listed below declare that they have no known competing financial interests or personal relationships that could have appeared to influence the work reported in this paper.

Acknowledgments

We thank David Rubilar-Rogers, Ivette Araya, Jhoann Canto, Javiera Leiva, Christian Becker, Francisco Garrido, Verónica Silva (MNHNCL), Guillermo D'Elía, Freddy Mondaca (IEEUACh), Michel Sallaberry, Juan Pablo Guevara, Luna Núñez (UCHZV), Patricio Zavala (SSUC), Diego Jara (Osteovet), Pedro Cárdenas (CEHA), Julián Faivovich, Paula Muzzopappa (MACN) and Douglas Jackson Squella for access to comparative collections. We also thank to Añañuca Foundation for its support. Finally, we thank to Julio Montané† and Lautaro Núñez, the archaeologists who obtained the fossils samples analyzed here. This research was partly funded through Fondecyt Grant #11170919 and Fondecyt Postdoctoral Grant #3170706 (NAV). JAM, FSL and SSA were supported by Proyecto Anillo (PIA-ANID, Chile) ACT-172099.

Appendix C. Supplementary data

Supplementary data to this article can be found online at https://doi.org/10.1016/j.quascirev.2020.106282.

References

Alarcón, J., 2016. Las aves fósiles de la Laguna de Tagua-Tagua. Undergraduate thesis, Universidad de Chile, Chile, p. 154.

Alberdi, M.T., Frassinetti, D., 2000. Presencia de *Hippidion* y *Equus* (*Amerhippus*) (Mammalia, Perissodactyla) y su distribución en el Pleistoceno superior de Chile. Estud. Geol. 56 (5–6), 279–290.

Alberdi, M.T., Prado, J.L., Cartelle, C., 2002. El registro de *Stegomastodon* (Mammalia Gomphotheriidae) en el Pleistoceno superior de Brasil. Rev. Esp. Palaontol. 17 (2), 217–235.

Alberdi, M.T., Cartelle, C., Prado, J.L., 2003. El registro Pleistoceno de *Equus* (*Amerhippus*) e *Hippidion* (Mammalia, Perissodactyla) de Brasil. Consideraciones paleoecológicas y biogeográficas. Ameghiniana 40, 173–196.

Albino, A.M., 1989. Primer registro de Colubroidea (Reptilia: Serpentes) de Argentina (Edad Montehermosense S.L, Plioceno). Ameghiniana 25 (3), 281–287.

Albino, A.M., 1999. Serpientes del sitio arqueológico Cueva Tixi (Pleistoceno tardío - holoceno), Provincia de Buenos Aires, Argentina. Ameghiniana 36, 269–273.

Alcaraz, M.A., 2010. Sistemática de los cérvidos (Mammalia, Artiodactyla) del Pleistoceno de las áreas extraandinas de Argentina. PhD Thesis. Universidad Nacional de La Plata, p. 317.

Alcaraz, M.A., Francia, A., 2013. Diversidad de Cervidae (Mammala: arctiodactyla) en el Pleistoceno de la Provincia de Corrientes, Argentina. Revista Brasilera de Paleontología 16 (1), 157–166. https://doi.org/10.4072/rbp.2013.1.12.

Andrews, P., 1990. Owls, Caves, and Fossils. University of Chicago Press, Chicago.

Azorit, C., Analía, M., Carrasco, R., Calvo, J.A., Muñoz-Cobo, J., 2002. Teeth eruption pattern in red deer (*Cervus elaphus hispanicus*) in southern Spain. An. Biol. 24, 107–114.

Bacigalupe, L.D., Rezende, E.L., Kenagy, G.J., Bozinovic, F., 2003. Activity and space use by degus: a trade-off between thermal conditions and food availability? J. Mammal. 84 (1), 311–318.

Barnosky, A.D., Lindsey, E.L., 2010. Timing of Quaternary megafaunal extinction in South America in relationto human arrival and climate change. Quat. Int. 217, 10–29. https://doi.org/10.1016/j.quaint.2009.11.017.

Barone, R., 1976. Anatomie comparée des mammifères domestiques. Tome 1. Ostéologie. Vigot freres, Paris.

Baumel, J., Witmer, L.M., 1993. Osteology. In: Baumel, J., King, A., Breazile, J.E., Evans, H., Vnaden Bergue, J.C. (Eds.), Handbook of Avian Anatomy. Nomina Anatomica Avium. Cambridge University Press, Cambridge, pp. 45–132.

Behrensmeyer, A.K., 1978. Taphonomic and ecologic information from bone weathering. Paleobiology 4 (2), 150–162.

Bever, G., 2005. Variation in the ilium of North American *Bufo* (Lissamphibia; Anura) and its implications for species-level identification of fragmentary anuran fossils. J. Vertebr. Paleontol. 25 (3), 548–560.

Binford, L.R., 1981. Bones: Ancient Men and Modern Myths. Academic Press, New York.

Bogan, D., de los Reyes, M.L., Cenizo, M.M., 2009. Primeros registros fósiles de pejerreyes (Teleostei: Atheriniformes) en el Pleistoceno Medio de la provincia de Buenos Aires, Argentina. Revista del Museo Argentino de Ciencias Naturales,

Nueva Serie 11 (2), 185–192. https://doi.org/10.22179/REVMACN.11.258.
Boles, W.E., 2005. A new flightless gallinule (aves: Rallidae: *Gallinula*) from the oligo-miocene of riversleigh, northwestern queensland, Australia. Record Aust. Mus. 57, 179–190.
Bozinovic, F., Ruíz, G., Cortés, A., Rosenmann, M., 2005. Energética, termorregulación y sopor en la yaca *Thylamys elegans* (Didelphidae). Rev. Chil. Hist. Nat. 78 (2), 199–206.
Brown, W.A.B., Chapman, N.G., 1990. The dentition of fallow deer (*Dama dama*): a scoring scheme to assess age from wear of the permanent molariform teeth. J. Zool. 221, 659–682.
Bulgarella, M., Wilson, R.E., Kopuchian, C., Valqui, T.H., McCracken, K.G., 2007. Elevational variation in body size of crested ducks (*Lophonetta specularioides*) from the central high andes, Mendoza, and Patagonia. Ornitol. Neotrop. 18, 587–602.
Camolez, T., Zaher, H., 2010. Levantamento, identificação e descrição da fauna de Squamata do Quaternario brasileiro (Lepidosauria). Arquivos de Zoologia, Museu de Zoologia da Universidade de São Paulo 41, 1–96.
Campbell, KEJr, 1973. The Pleistocene Fauna of the Talara Tar Seeps, Northwestern Peru. The University of Florida, Unpublished Thesis, pp. 1–239.
Cartajena, M.I., López, P., Carabias, D., Morales, C., Vargas, G., Ortega, C., 2013. First evidence of fan underwater Final Pleistocene terrestrial extinct faunal bone assemblage from central Chile (South America): taxonomic and taphonomic analyses. Quat. Int. 305, 45–55.
Casamiquela, R.M., 1972. Catalogación crítica de algunos vertebrados fósiles chilenos. II Los mastodontes. Ameghiniana 9 (3), 193–208.
Casamiquela, R.M., 1976. Los vertebrados fósiles de Tagua-Tagua. Actas del Primer Congreso Geológico Chileno Tomo I, C87–C102.
Casamiquela, R.M., 1999. The Pleistocene vertebrate record of Chile. Quat. S. Am. Antarct. Peninsula 7, 91–107.
Casamiquela, R.M., Sepúlveda, F., 1974. Catalogación crítica de algunos vertebrados fósiles chilenos. III. Los megaterioídeos. Sobre *Megatherium medinae* Philippi. Ameghiniana 11 (2), 97–123.
Cenizo, M.M., Tassara, D., 2013. Nuevos registros fósiles del halcón plomizo (*Falco femoralis* Temminck 1822; Falconidae) en el Pleistoceno del centro-este de Argentina. Revista Historia Natural. Tercera Serie 3 (1), 13–30.
Cenizo, M.M., Agnolin, F.L., Pomi, L.H., 2015. A new Pleistocene bird assemblage from the southern pampas (Buenos Aires, Argentina). Palaeogeogr. Palaeoclimatol. Palaeoecol. 420, 65–81.
Chéneval, J., Escuillié, F., 1992. New data concerning *Palaelodus ambiguus* (aves: phoenicopteriformes: palaelodidae): ecological and evolutionary interpretations. In: Campbell, K.E. (Ed.), Papers in Avian Paleontology Honoring Pierce Brodkorb. Los Angeles: Natural History Museum of Los Angeles Country, Science Series, vol. 36, pp. 208–224.
Cione, A.L., Tonni, E.P., Soibelzon, L., 2009. Did humans cause the late Pleistocene-early Holocene mammalian extinctions in South America in a context of shrinking open areas? In: Haynes, G. (Ed.), American Megafaunal Extinctions at the End of the Pleistocene. Springer, New York, pp. 125–144.
Cohen, A., Serjeantson, D., 1986. A Manual for the Identification of Bird Bones from Archaeological Sites. Jubilee Printers, London.
Correa, P., Roa, A., 2005. Relaciones tróficas entre *Oncifelis guigna, Lycalopex culpaeus, Lycalopex griseus* y *Tyto alba* en un ambiente fragmentado de la zona central de Chile. Mastozool. Neotrop. 12 (1), 57–60.
Couve, E., Vidal, C.F., Ruiz, J., 2016. Aves de Chile. Sus islas oceánicas y Península Antártica. Una guía de campo ilustrada. FS Editorial, Punta Arenas.
Covacevich, V., 1971. Los moluscos pleistocénicos y holocénicos de San Vicente de Taguatagua. Universidad de Chile, Santiago de Chile. Undergraduate Thesis.
De Mendoza, R., Tambussi, C., 2019. *Cayaoa bruneti* (aves: anseriformes) from the early miocene of Patagonia, Argentina: new materials and revised diagnosis. Ameghiniana 53 (3). https://doi.org/10.5710/AMGH.24.05.2019.3199.
Domingo, L., Prado, J.L., Alberdi, M.T., 2012. The effect of paleoecology and paleobiogeography on stable isotopes of Quaternary mammals from South America. Quat. Sci. Rev. 55, 103–113.
Domínguez-Rodrigo, M., 1999. Flesh availability and bone modification in carcasses consumed by lions. Palaeogeogr. Palaeoclimatol. Palaeoecol. 149, 373–388.
Donoso-Barros, R., 1966. Los reptiles de Chile. Editorial Universitaria, Santiago.
Dyer, B.S., 1997. Phylogenetic Revision of Atherinopsinae (Teleostei, Atherinopsidae), with Comments on the Systematics of the South American Freshwater Fish Genus Basilichthys Girard, vol. 185. Miscellaneous Publications Museum of Zoology, University of Michigan.
Ebensperger, L.A., Hurtado, M.J., 2005. On the relationship between herbaceous cover and vigilance activity of degus (*Octodon degus*). Ethology 111 (6), 593–608.
Eisenmann, V., Alberdi, M.T., de Giuli, C., Staesche, U., 1988. Studying Fossil Horses. E.J. Brill, Leiden, The Netherlands.
Falabella, F., Melendez, R., Vargas, L., 1995. Claves osteológicas para peces de Chile central, un enfoque arqueológico. Departamento de antropología Facultad de Ciencia Sociales, Universidad de Chile y Museo Nacional de Historia Natural.
Fernández, F.J., Ballejo, F., Moreira, G., Tonni, E., De Santis, L.J.M., 2011. Roedores cricétidos de la provincia de Mendoza. Guía cráneo-dentaria orientada para su aplicación en estudios zooarqueológicos. Sociedad Argentina de Antropología and Universitas Sarmiento Córdoba.
Fernández-Jalvo, Y., Andrews, P., 1992. Small mammal taphonomy of gran dolina, (atapuerca, Burgos, Spain). J. Archaeol. Sci. 19, 407–428.
Fernández-Jalvo, Y., Andrews, P., 2003. Experimental effects of water abrasion on bone fragments. J. Taphon. 1 (3), 147–163.
Fernández-Jalvo, Y., Andrews, P., 2016. Atlas of Taphonomic Identifications. 1001+ Images of Fossil and Recent Mammal Bone Modification. Springer, Vertebrate Paleobiology and Paleoanthropology. https://doi.org/10.1007/978-94-017-7432-1.
Fernández-Jalvo, Y., Tormoa, L., Andrews, P., Dolores Marin-Monfort, M., 2018. Taphonomy of burnt bones from Wonderwerk cave (South Africa). Quat. Int. 495, 19–29. https://doi.org/10.1016/j.quaint.2018.05.028.
Ferretti, M.P., 2010. Anatomy of *Haplomastodon chimborazi* (Mammalia, Proboscidea) from the late Pleistocene of Ecuador and its bearing on the phylogeny and systematics of South American gomphotheres. Geodiversitas 32 (4), 663–721.
Frassinetti, D., Alberdi, M.T., 2000. Revisión y estudio de los restos fósiles de mastodontes de Chile (Gomphotheriidae): *Cuvieronius hyodon*, Pleistoceno superior. Estud. Geol. 56 (3–4), 197–208.
Frison, G.C., Todd, L.C., 1986. The Colby Mammoth Site: Taphonomy and Archaeology of a Clovis Kill in Northern Wyoming. University of New Mexico Press, Albuquerque, New Mexico.
Froese, R., Pauly, D. (Eds.), 2019. FishBase. World Wide Web electronic publication. www.fishbase.org. accessed 04/2019.
Frost, D.R., Grant, T., Faivovich, J., Bain, R.H., Haas, A., Haddad, C.F.B., De Sá, R.O., Channing, A., Wilkinson, M., Donnellan, S.C., Raxworthy, C.J., Cambell, J.A., Blotto, B.L., Moller, R., Drewes, R.C., Nussbaum, R.A., Lynch, J.D., Green, D.M., Wheeler, W.C., 2006. The amphibian tree of life. Bull. Am. Mus. Nat. Hist. 297, 3–370.
Gallardo, M.H., Reise, D., 1992. Systematics of *Aconaemys* (Rodentia, Octodontidae). J. Mammal. 73 (4), 779–788.
Gidna, A., Kisui, B., Mabulla, A., Musiba, Ch, Domínguez-Rodrigo, M., 2014. An ecological neo-taphonomic study of carcass consumption by lions in Tarangire National Park (Tanzania) and its relevance for human evolutionary biology. Quat. Int. 322–323, 167–180.
Gifford-González, D., 1991. Bones are not enough: analogues, knowledge, and interpretive strategies in zooarchaeology. J. Anthropol. Archaeol. 10, 215–254.
Gilbert, B.M., Martin, L.D., Savage, H.G., 1981. Avian Osteology. Flagstaff.
Gill, F., Donsker, D. (Eds.), 2016. IOC World Bird List (V 6.2). https://doi.org/10.14344/IOC.ML.6.2.
Godoy, E., Schilling, M., Solari, M., Fock, A., 2009. Geología del área Rancagua-San Vicente de Tagua Tagua. Servicio Nacional de Geología y Minería, Chile.
Gómez, R.O., Turazzini, G.F., 2016. An overview of the ilium of anurans (Lissamphibia, Salientia), with a critical appraisal of the terminology and primary homology of main ilial features. J. Vertebr. Paleontol. 36 (1), 1–12. https://doi.org/10.1080/02724634.2015.1030023.
González-Guarda, E., Domingo, L., Tornero, C., Pino, M., Fernández, M.H., Sevilla, P., Villavicencio, N., Agustí, J., 2017. Late Pleistocene ecological, environmental and climatic reconstruction based on megafauna stable isotopes from northwestern Chilean Patagonia. Quat. Sci. Rev. 170, 188–202.
González-Guarda, E., Petermann-Pichincura, A., Tornero, C., Domingo, L., Agustí, J., Pino, M., Abarzúa, A.M., Capriles, J.M., Villavicencio, N., Labarca, R., Tolorza, V., Sevilla, P., Rivals, F., 2018. Multiproxy evidence for leaf-browsing and closed habitats in extinct proboscideans (Mammalia, Proboscidea) from Central Chile. Proc. Natl. Acad. Sci. Unit. States Am. 115 (37), 9258–9263.
Gosner, K.L., 1960. A simplified table for staging anuran embryos and larvae with notes on identification. Herpetologica 16, 183–190.
Gracian-Negrete, J.M., González-Acosta, A.F., González-Isáis, M., Ortiz-Galindo, J.L., Del Moral-Flores, L.F., 2012. Osteología comparada del esqueleto caudal de *Achirus lineatus* y *Achirus mazatlanus* (Pleuronectiformes: achiridae). Int. J. Morphol. 30 (2), 705–708.
Grayson, D., 1984. Quantitative Zooarchaeology. Academic Press, Orlando.
Grazziotin, F.G., Zaher, H., Murphy, R.W., Scrocchi, G., Benavides, M.A., Zhang, Y.-P., Bonatto, S.L., 2012. Molecular phylogeny of the new World dipsadidae (Serpentes: colubroidea): a reappraisal. Cladistics 28, 437–459.
Gregory, W.K., Conrad, G.M., 1937. The comparative osteology of the swordfish (*Xiphias*) and the sailfish (*Istiophorus*). Am. Museum of Natl. Hist. 952, 1–28.
Griffith, S.J., Thompson, C.E.L., Thompson, S.J.U., Gowland, R.L., 2016. Experimental abrasion of water submerged bone: the influence of bombardment by different sediment classes on microabrasion rate. J. Archaeol. Sci.: Rep. 10, 15–29. https://doi.org/10.1016/j.jasrep.2016.09.001.
Haynes, G., 1987. Elephant-butchering at modern mass-kill sites in Africa. Curr. Res. Pleistocene 4, 75–77.
Haynes, G., 1991. Mammoths, Mastodonts, and Elephants: Biology, Behavior, and the Fossil Record. Cambridge University Press, Cambridge.
Haynes, G., Klimowicz, J., 2015. Recent elephant-carcass utilization as a basis for interpreting mammoth exploitation. Quat. Int. 359 (360), 19–37.
Hershkovitz, P., 1967. Dynamics of rodent molar evolution: a study based on New World Cricetinae, family Muridae. J. Dent. Res. 46 (5), 829–842.
Hesse, B., 1984. Archaic exploitation of small mammals and birds in Northern Chile. Estud. Atacameños 4, 42–61.
Heusser, C.J., 1983. Quaternary pollen records from Laguna de Tagua-Tagua, Chile. Science 219, 1429–1432.
Heusser, C.J., 1990. Ice age vegetation and climate of subtropical Chile. Palaeogeogr. Palaeoclimatol. Palaeoecol. 80, 107–127.
Hill, A., 1979. Disarticulation and scattering of mammalian skeletons. Paleobiology 5 (3), 261–274.
Hoffstetter, R., 1968. Naupa, un gisement de vertebres Pleistocene dans le chaco Bolivien. Bull. Mus. Natl. Hist. Nat. 40, 823–836.
Hogg, A.G., Hua, Q., Blackwell, P.G., Niu, M., Buck, C.E., Guilderson, T.P., Heaton, T.J., et al., 2013. SHCal13 Southern Hemisphere calibration, 0–50,000 years cal BP. Radiocarbon 55 (4), 1889–1903.

Holman, J.A., 2000. The Fossil Snakes of North America. Indiana University Press, Indianapolis.
Hutterer, R., 1994. Island rodents: a new species of *Octodon* from Isla Mocha, Chile (Mammalia: Octodontidae). Zeitschrift für Säugetierkunde 59 (1), 27–41.
Iriarte, A., 2008. Mamíferos de Chile. Lynx Ediciones, Barcelona.
Jackson, D., Aspillaga, E., Rodríguez, X., Jackson, D., y Méndez, F., Santana, C., 2012. Las Ocupaciones Humanas del Sitio Arqueológico de Santa Inés, Laguna de Tagua Tagua, Chile Central. Rev. Antropol. 26, 151–168.
Jaksic, F., Schlatter, R., Yáñez, J., 1980. Feeding ecology of central Chilean foxes, *Dusicyon culpaeus* and *Dusicyon griseus*. J. Mammal. 61, 254–260.
Jaramillo, A., 2005. Aves de Chile. Lynx Edicions, Barcelona.
Kaiser, J., Lamy, F., Hebbeln, D., 2005. A 70-kyr sea surface temperature record of southern Chile (Ocean Drilling Program Site 1233). Paleoceanography 20 (4), PA4009. https://doi.org/10.1029/2005PA001146.
Kaiser, J., Schefuß, E., Lamy, F., Mohtadi, M., Hebbeln, D., 2008. Glacial to Holocene changes in sea surface temperature and coastal vegetation in north central Chile: high versus low latitude forcing. Quat. Sci. Rev. 27 (21–22), 2064–2075.
Kenagy, G.J., Nespolo, R.F., Vásquez, R.A., Bozinovic, F., 2002. Daily and seasonal limits of time and temperature to activity of degus. Rev. Chil. Hist. Nat. 75 (3), 567–581.
Labarca, R., 2015. La Meso y Megafauna extinta del Pleistoceno de Chile. Publicación Ocasional del Museo Natl. .Hist. Natl. Chile 63, 401–465.
Labarca, R., 2016. La subsistencia de los cazadores recolectores de Patagonia meridional chilena durante la transición Pleistoceno – Holoceno: un enfoque integrador desde la zooarqueología. PhD Thesis. Universidad del Centro de La Provincia de Buenos Aires, Argentina, p. 468.
Labarca, R., 2020. Taphonomy of the pilauco site, northwestern Chilean Patagonia. In: Pino, M., Astorga, G. (Eds.), Pilauco: a Late Archaeo-Paleontological Site. Osorno, Northwestern Patagonia and Chile. Springer Nature Switzerland, The Latin American Studies Book Series, pp. 123–156.
Labarca, R., Alberdi, M.T., 2011. An updated taxonomic view on the family Gomphotheriidae (Proboscidea) in the final Pleistocene of south central Chile. Neues Jahrbuch Geol. Palaontol. Abhand. 262 (1), 43–57.
Labarca, R., Alcaraz, M.A., 2011. Presencia de *Antifer ultra* Ameghino (=*Antifer niemeyer*i Casamiquela) (Artiodactyla, Cervidae) en el Pleistoceno tardío-Holoceno temprano de Chile central (30-35°S). Andean Geol. 38 (1), 156–170.
Labarca, R., Alberdi, M.T., Prado, J.L., Mansilla, P., Mourgues, F.A., 2016. Nuevas evidencias acerca de la presencia de *Stegomastodon platensis*, Ameghino, 1988, Proboscidea Gomphotheriidae en el Pleistoceno Tardío de Chile central. Estud. Geol. 76 (1), e046. https://doi.org/10.3989/egeol.42199.385.
Lagos, V.O., Bozinovic, F., Contreras, L.C., 1995. Microhabitat use by a small diurnal rodent (*Octodon degus*) in a semiarid environment: thermoregulatory constraints or predation risk? J. Mammal. 76 (3), 900–905.
Lamy, F., Hebbeln, D., Wefer, G., 1999. High-resolution marine record of climatic change in mid-latitude Chile during the last 28,000 years based on terrigenous sediment parameters. Quat. Res. 51, 83–93.
Lara, L.E., Wall, R., Stockli, D., 2008. La ignimbrita Pudahuel (Asociación Piroclástica Pumícea) y la Caldera Diamante (33°S): Nuevas edades U-Th-He. Actas del XVII Congreso Geológico Argentino, Jujuy.
Lira, M.P., Labarca, R., Fritte, D., Oyarzo, H., Pino, M., 2020. The site Los Notros: geology and first taxonomic descriptions. In: Pino, M., Astorga, G. (Eds.), Pilauco: a Late Archaeo-Paleontological Site. Osorno, Northwestern Patagonia and Chile. Springer Nature Switzerland, The Latin American Studies Book Series, pp. 231–248.
Lloveras, L., Moreno-García, M., Nadal, J., 2009. Butchery, cooking and human consumption marks on rabbit (*Oryctolagus cuniculus*) bones: an experimental study. J. Taphon. 7 (2–3), 179–201.
López, P., Cartajena, M.I., Carabias, D., Prevosti, F.J., Maldonado, A., Flores-Aqueveque, V., 2016. Reconstructing drowned terrestrial landscapes. Isotopic paleoecology of a late Pleistocene extinct faunal assemblage: site GNL Quintero 1 (GNLQ1) (32° S, Central Chile). Quat. Int. https://doi.org/10.1016/j.quaint.2016.08.017.
Lyman, R.L., 1994. Vertebrate Taphonomy. Cambridge Manuals in Archaeology. Cambridge University Press.
Lyman, R.L., 2008. Quantitative Paleobiology. Cambridge Manuals in Archaeology. Cambridge University Press.
Lynch, J.D., 1971. Evolutionary Relationships, Osteology, and Zoogeography of Leptodactyloid Frogs. University of Kansas, Lawrence.
Manegold, A., Pavia, M., Haarhoff, P., 2014. A new species of *Aegypius* vulture (Aegypiinae, Accipitridae) from the early Pliocene of South Africa. J. Vertebr. Paleontol. 34 (6), 1394–1407.
Marean, C.W., Ehrhardt, C.L., 1995. Paleoanthropological and paleoecological implications of the taphonomy of a sabertooth's den. J. Hum. Evol. 29 (6), 515–547.
Marín-Arroyo, A.B., Landete-Ruiz, M.D., Vidal-Bernabeu, G., Seva-Román, R., González-Morales, M., Straus, L.G., 2008. Archaeological implications of human-derived manganese coatings: a study of blackened bones in El Mirón Cave, Cantabrian Spain. J. Archaeol. Sci. 35 (3), 801–813.
Marín-Arroyo, A.B., Landete-Ruiz, M.D., Seva-Román, R., Lewis, M.D., 2014. Manganese coating of the Tabun faunal assemblage: implications for modern human behaviour in the Levantine Middle Palaeolithic. Quat. Int. 330, 10–18. https://doi.org/10.1016/j.quaint.2013.07.016.
Martin, F.M., 2013. Tafonomía y paleoecología de la transición Pleistoceno-Holoceno en Fuego Patagonia. Interacción entre humanos y carnívoros y su importancia como agentes en la formación del registro fósil. Ediciones de la Universidad de Magallanes, Punta Arenas.
Martínez-Piña, D., González-Cifuentes, G., 2017. Aves de Chile. Guía de Campo y Breve Historia Natural. Ediciones del Naturalista, Santiago.
Mayr, G., 2004. Morphological evidence for sister group relationship between flamingos (Aves: phoenicopteridae) and grebes (Aves: Podicipedidae). Zool. J. Linn. Soc. 140, 157–169.
Méndez, C., 2015. Los Primeros Andinos. Tecnología Lítica de los Habitantes del Centro de Chile Trece Mil Años Atrás. Fondo Editorial Pontificia Universidad Católica del Perú, Lima.
Mengoni-Goñalons, G.L., 1999. Cazadores de Guanacos de la estepa Patagónica. Colección tesis doctorales. Sociedad Argentina de Antropología.
Metcalfe, J.Z., Longstaffe, F.J., Hodgins, G, 2013. Proboscideans and paleoenvironments of the Pleistocene Great Lakes: landscape, vegetation, and stable isotopes. Quaternary Science Reviews 76, 102–113. https://doi.org/10.1016/j.quascirev.2013.07.004.
Montané, J., 1968. Paleo-Indian remains from Laguna de Tagua Tagua, Central Chile. Science 161 (3846), 1137–1138.
Moreno, P.I., Lowell, T.V., Jacobson, G.L., Denton, G.H., 1999. Abrupt vegetation and climate changes during the last glacial maximum and last Termination in the Chilean lake district: a case study from canal de la Puntilla (41S). Geogr. Ann. 81 A, 285–311.
Moreno, P.I., Videla, J., Valero-Garcés, B., Alloway, B.V., Heusser, L.E., 2018. A continuous record of vegetation, fire-regime and climatic changes in north western Patagonia spanning the last 25,000 years. Quat. Sci. Rev. 198, 15–36.
Mothé, D., Avilla, L.S., Winck, G.R., 2010. Population structure of the gomphothere *Stegomastodon waringi* (mammalia: proboscidea: Gomphotheriidae) from the Pleistocene of Brazil. Annais da Academia Brasileria de Ciencias 82 (4), 983–996.
Mothé, D., Avilla, L.S., Asevedo, L., Borges-Silva, L., Rosas, M., Labarca, R., Souberlich, R., Soibelzon, E., Román-Carrión, J.L., Ríos, S.D., Rincón, A.D., Cardoso de Oliveira, G., Pereira Lopes, R., 2017. Sixty years after 'The mastodonts of Brazil': the state of the art of South American proboscideans (Proboscidea, Gomphotheriidae). Quat. Int. 443 (Part A), 52–64. https://doi.org/10.1016/j.quaint.2016.08.028.
Muzzopappa, P., Pugener, L.A., Baez, A.M., 2016. Postcranial osteogenesis of the helmeted water Toad *Calyptocephalella gayi* (Neobatrachia: Calyptocephalellidae) with comments on the osteology of australobatrachians. J. Morphol. 277, 204–230.
Navas, J.R., Bo, N.A., 1998. The geographical distribution of the subspecies of *Lophonetta specularioides* and *Merganetta armatta* (Anatidae) in the provinces of Mendoza and San Juan, Argentina. Hornero 15, 57–59.
Nicholson, R.A., 1996. Bone degradation, burial medium and species representation: debunking the myths, an experiment-based approach. J. Archaeol. Sci. 23, 513–533. https://doi.org/10.1006/jasc.1996.0049.
Noriega, J.I., Areta, J.I., Vizcaíno, S.F., Bargo, M.S., 2011. Phylogeny and taxonomy of the patagonian miocene falcon *Thegornis musculosus* ameghino, 1895 (aves: Falconidae). J. Paleontol. 85 (6), 1089–1104.
Núñez, L., Varela, J., Casamiquela, R., Schiappacasse, V., Niemeyer, H., Villagrán, C., 1994. Cuenca de Taguatagua en Chile: el ambiente del Pleistoceno superior y ocupaciones humanas. Rev. Chil. Hist. Nat. 67, 503–519.
Osgood, W.H., 1943. The Mammals of Chile. Field Museum of Natural History.
Otero, R.A., Jiménez-Huidobro, P., Soto-Acuña, S., Yury-Yáñez, A.E., 2014. Evidence of a giant helmeted frog (australobatrachia, Calyptocephalellidae) from eocene levels of the magallanes basin, southernmost Chile. J. S. Am. Earth Sci. 55 (2014), 133–140.
Palma, J., 1969. El sitio de Tagua-Tagua en el ámbito paleo- americano. In: Actas del Quinto Congreso Nacional de Arqueología. Museo Arqueológico de La Serena, La Serena, Chile, pp. 315–325.
Palma, R.E., 1997. Thylamys elegans. Mamm. Species 572, 1–4.
Parker, W.K., 1881. On the structure and development of the skull in the Batrachia. Part III Philos. Trans. Roy. Soc. Londn. 172, 1–266.
Patton, J.L., Pardiñas, U.F., D'Elía, G. (Eds.), 2015. Mammals of South America, Volume 2: Rodents, vol. 2. University of Chicago Press.
Pesquero, M.D., Ascaso, C., Alcalá, L., Fernández-Jalvo, Y., 2010. A new taphonomic bioerosion in a Miocene lakeshore environment. Palaeogeogr. Palaeoclimatol. Palaeoecol. 295, 192–198. https://doi.org/10.1016/j.palaeo.2010.05.037.
Porta, J., 1965. Nota preliminar sobre la fauna de vertebrados hallada en Curití (Departamento de Santander, Colombia). Bol. Geol. 19, 112–115.
Prado, J.L., Alberdi, M.T., 2017. Fossil horses of South America phylogeny, systemics and ecology. In: The Latin American Studies Book Series. Springer.
Prado, J.L., Martinez-Maza, C., Alberdi, M.T., 2015. Megafauna extinction in south America: a new chronology for the argentine pampas. Palaeogeogr. Palaeoclimatol. Palaeoecol. 425, 41–49. https://doi.org/10.1016/j.palaeo.2015.02.026.
Prum, R.O., Berv, J.S., Dornburg, A., Field, D.J., Townsend, J.P., Lemmon, E.M., Lemmon, A.R., 2015. A comprehensive phylogeny of birds (Aves) using targeted next-generation DNA sequencing. Nature 526, 569–573.
Rage, J.C., 1984. Serpentes. In: Wellnhofer, P. (Ed.), Handbuch der Paläoherpetologie, Part 11. Fischer Verlag, Stuttgart, G, pp. 1–80.
Reinbach, W., 1939. Untersuchungen über die Entwicklung des Kopfskeletts von *Calyptocephalus gayi*. Jenaische Zeitschrift Für Naturwissencschaft 72, 211–362.
Reise, D., 1973. Clave para la determinación de los cráneos de marsupiales y roedores chilenos. Instituto de Biología, Universidad de Concepción.
Remsen, J.V., Areta, J.I., Bonaccorso, E., Claramunt, S., Jaramillo, A., Pacheco, J.F., Ribas, C., Robbins, M.B., Stiles, F.G., Stotz, D.F., Zimmer, K.J., 2020. A Classification of the Bird Species of South America. American Ornithological Society. http://www.museum.lsu./~Remsen/SACCBaseline.htm.

Saavedra, B., Simonetti, J.A., 2003. Holocene distribution of octodontid rodents in central Chile. Rev. Chil. Hist. Nat. 76 (3), 383–389.
Scanferla, C.A., Cenizo, M., de los Reyes, M., 2005. Sobre el primer registro fósil del género *Lystrophis* Cope, 1885 (Serpentes-Colubridae-Xenodontinae). Stud. Geol. Salmant. 41, 93–101.
Shaffer, B.S., Sánchez, J.L., 1994. Comparison of 1/8"- and 1/4"- mesh recovery of controlled samples of small-to-medium-sized mammals. Am. Antiq. 59, 525–530.
Shipman, P., Fosterb, G., Schoeninger, M., 1984. Burnt bones and teeth: an experimental study of color, morphology, crystal structure and shrinkage. J. Archaeol. Sci. 11, 301–325.
Silva, JLL da, 2008. Reconstituição paleoambiental baseada no estudo de mamíferos pleistocênicos de Maravilha e Poço das Trincheiras, Alagoas, nordeste do Brasil. PhD Thesis. Universidade Federal de Pernambuco, Recife, p. 244.
Silver, I.A., 1963. The ageing of domestic animals. In: Brothwell, D., Higgs, E. (Eds.), Science in Archaeology. Basic Books, New York, pp. 251–268.
Soto-Huenchumán, P., 2018. Estratigrafía y paleontología del Jurásico superior - Cretácico inferior del Cordón Norte de la Laguna de Tagua tagua (entre 34° 16' – 71° 10' y 34° 30' – 71° 05'), Comuna de San Vicente de tagua Tagua, Región del Libertador General Bernardo O'Higgins. Undergraduate thesis, Universidad Andrés Bello, Chile.
Stahl, P., 1996. The recovery and interpretation of microvertebrate bone assemblages from archaeological contexts. J. Archaeol. Method Theor 3 (1), 31–75.
Stewart, K.M., 1991. Modern fishbone assemblages at Lake Turkana, Kenya: a methodology to aid in recognition of hominid fish utilization. J. Archaeol. Sci. 18 (5), 579–603. https://doi.org/10.1016/0305-4403(91)90054-S.
Stuiver, M., Reimer, P.J., Reimer, R.W., 2019. CALIB 7.1 [WWW program] at. http://calib.org. (Accessed 6 September 2019).
Suazo-Lara, F., Fernández-Jiménez, R., Soto-Acuña, S., Manríquez, L., Alarcón-Muñoz, J., Aravena, B., Vargas, A.O., Leppe, M., 2017. Primer registro de Calyptocephalellidae (Anura, Australobatrachia) en el Cretácico Superior de Chile. I Reunión de Paleontología de Vertebrados de Chile, Santiago, p. 16.
Suazo-Lara, F., Alarcón-Muñoz, J., Fernández-Jiménez, R., Kaluza, J., Manríquez, L., Milla, V., Soto-Acuña, S., Leppe, M., 2018. Nuevos registros de anuros del Valle del Río de Las Chinas (Formación Dorotea, Cretácico Superior), Región de Magallanes, Chile. I Congreso Chileno de Paleontología, Punta Arenas – Puerto Natales, pp. 244–246.
Tercerie, S., Béarez, P., Pruvost, P., Bailly, N., Vignes-Lebbe, R., 2016. Osteobase. World Wide Web Electronic Publication. http://osteobase.mnhn.fr/. accessed 06/2019.
Teta, P.V., 2013. Relaciones filogenéticas de la tribu Abrotrichini (Rodentia, Cricetidae): análisis separados y combinados de evidencias morfológicas y moleculares. PhD Thesis. Facultad de Ciencias Naturales y Museo, Universidad Nacional de La Plata.
Tihen, J.A., 1962. Osteological observations on new World *Bufo*. Am. Midl. Nat. 67 (1), 157–183.
Tonni, E.P., 1969. La presencia de *Anas leucophrys* (Aves: anseriformes) en sedimentos de edad Ensenadense (Pleistoceno medio) de la provincia de Buenos Aires. Ameghiniana 6, 256–294.
Torres, N., 2007. Dieta estival del Culpeo (*Pseudalopex culpaeus,* Molina 1782) en Nevados de Chillán, Centro-Sur de Chile. Undergraduate Thesis. Universidad Austral de Chile.
Valdovinos, C., 2006. Estado de conocimiento de los Gastrópodos dulceacuícolas de Chile. Gayana 70 (1), 88–95. https://doi.org/10.4067/S0717-65382006000100014.
Valero-Garcés, B., Jenny, B., Rondanelli, M., Delgado-Huertas, A., Burns, S., Veit, H., Moreno, A., 2005. Palaeohydrology of Laguna de Tagua Tagua (34° 30' S) and moisture fluctuations in Central Chile for the last 46.000 yr. J. Quat. Sci. 20 (7–8), 625–641.
Varela, J., 1976. Estudio estratigráfico-sedimentológico de los depósitos de Laguna de Tagua-Tagua, provincia de O'Higgins. Undergraduate thesis. Universidad de Chile, p. 200.
Verzi, D.H., Quintana, C.A., 2005. The caviomorph rodents from the San Andrés Formation, east-central Argentina, and global Late Pliocene climatic change. Palaeogeogr. Palaeoclimatol. Palaeoecol. 219 (3–4), 303–320.
Victoriano, P.F., González, A.L., Schlatter, R., 2006. Estado de conocimiento de las aves de aguas continentales de Chile. Gayana 70 (1), 140–162.
Villagrán, C., Armesto, J.J., 1993. Full and late glacial paleoenvironmental scenarios for the West coast of southern South America. In: Mooney, H.A., Fuentes, E.R., Kronberg, B.I. (Eds.), Earth System Responses to Global Change: Contrasts between North and South America. Academic Press, San Diego, pp. 195–207.
Villagrán, C., Varela, J., 1990. Palynological evidence for increased aridity on the central Chilean coast during the Holocene. Quat. Res. 34, 198–207.
Woolfenden, G.E., 1961. Postcranial osteology of waterfowl. Bull. Florida State Museum 6, 1–129.
Woolfender, G.E., 1960. Osteology of the Waterfowl. PhD Thesis. University of Florida.
Worthy, T.F., 2004. The Holocene fossil waterfowl fauna of the lake pukawa, north island, New Zealand. TUHINGA 15, 75–120.
Worthy, T.F., Wragg, G.M., 2008. A new genus and species of pigeon (aves: Columbidae) from henderson island, Pitcairn group. Terra Aust. 29, 419–510.
Worthy, T.H., Tennyson, A.J.D., Jones, C., McNamara, J.A., Douglas, B.J., 2007. Miocene waterfowl and other birds from central Otago, New Zealand. J. Syst. Palaeontol. 5 (1), 1–39.
Zaher, H., Grazziotin, F.G., Cadle, J.E., Murphy, R.W., Moura-Leite, J.C., Bonatto, S.L., 2009. Molecular phylogeny of advanced snakes (Serpentes, Caenophidia) with an emphasis on South American Xenodontines: a revised classification and descriptions of new taxa. Papéis Avulsos Zool. (São Paulo) 49, 115–153.
Zaher, H., Murphy, R.W., Arredondo, J.C., Graboski, R., Machado-Filho, P.R., Mahlow, K., Montingelli, G.G., Bottallo Quadros, A., Orlov, N.L., Wilkinson, M., Zhang, Y.P., Grazziotin, G., 2019. Large-scale molecular phylogeny, morphology, divergence-time estimation, and the fossil record of advanced caenophidian snakes (Squamata: Serpentes). PloS One 14 (5), e0216148.
Zelenkov, N.V., 2010. Diving ducks from the middle miocene of western Mongolia. Paleontol. J. 45 (2), 191–199.
Zelenkov, N.V., Kurochkin, E.N., 2012. Dabbling ducks (aves: Anatidae) from the middle miocene of Mongolia. Paleontol. J. 46 (4), 421–429.
Zohar, I., Belmaker, M., 2005. Size does matter: methodological comments on sieve size and species richness in fishbone assemblages. J. Archaeol. Sci. 32 (4), 635–641. https://doi.org/10.1016/S0305-4403(03)00037-2.